Long-term impact of wastewater effluent discharge on groundwater: identification of contaminant plume by geochemical, isotopic, and organic tracers' approach

Antoine Bonnière, Somar Khaska, Corinne Le Gal La Salle, Pascale Louvat, Patrick Verdoux

Water Research 257 (2024) 121637

Contents lists available at ScienceDirect

Water Research

journal homepage: www.elsevier.com/locate/watres

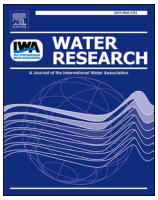

Long-term impact of wastewater effluent discharge on groundwater: Identification of contaminant plume by geochemical, isotopic, and organic tracers' approach

A. Bonnière [a,*], S. Khaska [a], C. Le Gal La Salle [a], P. Louvat [b,c], P. Verdoux [a]

[a] UPR CHROME, Université de Nîmes, F-30021 Nîmes CEDEX 1, France
[b] Université Paris Cité, Institut de Physique du Globe de Paris, CNRS, UMR 7154, Paris, France
[c] Université de Pau et des Pays de l'Adour, E2S UPPA, CNRS, IPREM, UMR 5254, Pau, France

ARTICLE INFO

Keywords:
Groundwater contamination
Wastewater contamination
Environmental tracers
Contaminants of emerging concern (CECs)
Gadolinium (Gd)

ABSTRACT

Infiltration of effluents from wastewater treatment plants (WWTP) into groundwater can be a source of Contaminants of Emerging Concern (CECs), such as pharmaceutical compounds, that are not fully removed during the treatment processes. A multi-tracer approach, based on hydrogeochemical, isotopic, and organic tracers, is applied in the Vistrenque Aquifer (Gard, France) to assess the dispersion of such unintentional plumes and its potential implication on groundwater quality for CECs in a small catchment area. In this area, a point source of WWTP effluent causes contaminant infiltration and unintentional transfer to the aquifer. This strong impact of an urban effluent was revealed from the Br/Cl ratio, boron concentrations and $\delta^{11}B$ isotopic signature of the groundwater in the direct vicinity of the infiltration point. With increasing distance from that point, dilution with groundwater rapidly attenuates the urban signal from these hydrogeochemical and isotopic tracers. Nevertheless, a gadolinium anomaly, resulting from discharges of urban wastewater containing the contrast agents used for magnetic resonance imaging (MRI), highlights the presence of a wastewater plume further along the flow line, that comes with a series of organic molecules, including pharmaceutical residues. Monitoring persistent or reactive molecules along the plume provides a more detailed understanding of the transfer of CECs into groundwater bodies. This highlights the relevance of pharmaceutical compounds as co-tracers for WWTP plume delineation. The present multi-tracer approach for groundwater resource vulnerability towards CECs allows a more in-depth understanding of contaminant transfer and their fate in groundwater.

1. Introduction

The ever-increasing demand for groundwater supply (drinking water, agriculture, industry) in the context of climate change (precipitation regimes, evapotranspiration, and river flows) is a rising concern for the quantity and quality of the water resource (Green et al., 2011; Kumar, 2012; IPCC, 2023). To address this concern, the reuse of treated water from Wastewater Treatment Plants (WWTP) either for direct irrigation in agriculture or for artificial recharge of groundwater is considered (Misra, 2014; Jarraya-Horriche et al., 2020; Hassan et al., 2023). However, groundwater is a vulnerable resource subject to various sources of contamination (Burri et al., 2019), which can be derived from either agricultural activity (e.g., nitrates, pesticides), urban effluents (e.g., pharmaceutical compounds, multidrug-resistant bacteria) or industrial processes (e.g., per-and polyfluoroalkyl substances PFAS). WWTP are known to be a significant source of pharmaceutical compounds in the environment due to their incomplete removal during the treatment process. The efficiency of the pharmaceuticals' removal can range from 0 % to 90 %, depending on the specific compounds and on the treatment process employed, with average remaining concentrations of pharmaceutical compounds in the WWTP effluent ranging from a few ng/L^{-1} to several mg/L^{-1} (Kasprzyk-Hordern et al., 2009; Verlicchi et al., 2012; Blair et al., 2015; Archer et al., 2017; Mansouri et al., 2021).

Contaminants of Emerging Concern (CECs) are defined as substances for which there is generally no regulation requiring monitoring or public reporting of their presence in surface water, groundwater, or wastewater (Morin-Crini et al., 2022). These contaminants may represent a potential

* Corresponding author.
E-mail addresses: antoine.bonniere@unimes.fr, a.bonniere@pm.me (A. Bonnière).

https://doi.org/10.1016/j.watres.2024.121637
Received 30 November 2023; Received in revised form 11 April 2024; Accepted 16 April 2024
Available online 17 April 2024

risk for human health and the environment, with some of them acting as endocrine disruptors and potentially causing effects on aquatic organisms, even at low levels of exposure (US EPA, 2008, 2012). They include pharmaceutical compounds, personal care products and cosmetics, industrial substances, rare-earth elements (REE) & metallic trace elements (MTEs), pesticides, or biological agents. The transfer of such contaminants from surface waters (treated or raw urban effluent) to the groundwater reservoir has been highlighted in several studies (Cary et al., 2013; K'oreje et al., 2016; Lee et al., 2019; McCance et al., 2020). To assess the risks associated with these emerging contaminants, quantification of pharmaceutical compounds has been carried out in the WWTP influent or effluent (Kasprzyk-Hordern et al., 2009; Khasawneh and Palaniandy, 2021), the surface water (Wilkinson et al., 2022), and the groundwater (Lopez et al., 2015; Sui et al., 2015; Li et al., 2021). CECs' transfer in the environment is complex, due to the diversity of substances and their specific characteristics. The persistence of some compounds, such as carbamazepine, is well documented (Clara et al., 2004; Grossberger et al., 2014; Hai et al., 2018). However, other organic contaminants may be more or less persistent, showing different rates of retention or degradation during their transfer, through processes such as sorption, photo-oxidation, complexation reactions, or mixing (Lapworth et al., 2012; Blair et al., 2015; Kiecak et al., 2019).

Once in the groundwater, a set of geochemical tools can be used to monitor and quantify the WWTP effluent discharge within the aquifer. Concentrations of major and minor ions have proven to be reliable tracers, especially when a large series of temporal data is available (Bi et al., 2021; McCance et al., 2021). However, when the signatures of several sources are overlapping, this data alone is not sufficient, and co-tracers are used to disentangle the sources. The combination of nitrogen stable isotope ratios of nitrates and of boron isotope ratios has proven to be efficient to distinguish between organic fertilizers and wastewater effluent when both sources are present in the same study area (Widory et al., 2005; Briand et al., 2013, 2017; Adebowale et al., 2019). These tracers are often advertised for this type of investigation. However, boron has a high geochemical reactivity and may suffer isotopic fractionation depending on the pH, the temperature, the presence of clay minerals or organic matter (Schmitt et al., 2012; Gaillardet and Lemarchand, 2018; Chalk, 2020). Similarly, the use of stable isotopes of nitrogen requires the identification of the isotopic signature of the different nitrate sources and the denitrification processes likely to modify these signatures. Isotopic signatures of sulphate $\delta^{34}S/\delta^{18}O\text{-}SO_4^{2-}$ may also be used to assess groundwater contamination by wastewaters (Torssander et al., 2006; Jakóbczyk-Karpierz and Ślósarczyk, 2022). Isotopic tracers require a thorough understanding of the local biogeochemical processes and in-depth investigations. Unconventional tracers, such as the emerging contaminants themselves, can be used as tracers of groundwater contaminated by urban effluents (Cary et al., 2013; Van Stempvoort et al., 2013; Lapworth et al., 2018; McCance et al., 2020; Sérodes et al., 2021; Currell et al., 2022). For instance, carbamazepine is an antiepileptic which has been used as a conservative environmental tracer in several studies, due to its persistence in the environment (Clara et al., 2004; Gasser et al., 2010; Cary et al., 2013). In some cases, the use of microbiological indicators can be useful to identify the septic tanks or WWTP effluents (Katz et al., 2009; Briand et al., 2013, 2017), but their use may be limited in groundwater due to the attenuation capacity of the aquifer matrix (Li et al., 2015). Finally, some tracers such as gadolinium are usually used to assess urban wastewater discharge in surface waters but can also be detected in groundwaters (Knappe et al., 2005; Kulaksız and Bau, 2011; Brünjes et al., 2016; Johannesson et al., 2017; Boester and Rüde, 2020). Gadolinium chelates are used as contrast agents in magnetic resonance imaging (MRI). These chelates are very stable and are not supposed to be metabolized by the human body. The excreted molecules are not processed nor degraded by conventional WWTP (Lawrence et al., 2009; Boester and Rüde, 2020) and can be found in the aquatic environment (Rabiet et al., 2009; Lawrence and Bariel, 2010; Kulaksız and Bau, 2011; Merschel et al., 2015; Hatje et al., 2016). Gadolinium can be used as a conservative tracer for anthropogenic input of WWTP effluent in the hydrological cycle (Möller et al., 2000; Ebrahimi and Barbieri, 2019). While promising, as has been shown with its application in surface water, gadolinium is rarely used as a tracer for urban effluents in groundwater.

In this article, we explore the potential tracers that can be used to detect weak signals of the first signs of contamination in drinking water supply wells. We address this issue by investigating the spatial extent of a treated WWTP effluent plume in a small catchment area based on a multi-tracer approach. A selection of typical tracers of WWTP effluents is chosen, including hydrogeochemical tracers (Cl^-, PO_4^{3-}, Br/Cl, B, Gd), stable boron isotopes ($\delta^{11}B$), and pharmaceutical compounds. The study area is located in a zone where agricultural activities and sources of urban effluents are present. The tracers were therefore selected to track only urban effluents and their associated emerging contaminants. Other tracers such as NO_3^- or $\delta^{15}N/\delta^{18}O\text{-}NO_3^-$ are excluded from this study as they are heavily influenced by agricultural activities. We propose a critical assessment of the efficiency of the selected tracers to delineate the WWTP effluent plume extent. The aim of the present research is to increase our knowledge of the occurrence, fate, and tracing methods for emerging contaminants.

2. Site setting

2.1. Geological setting

The Vistrenque aquifer is located in the South of France. With a 325 km^2 surface area, approximately 14 million m^3/y is abstracted for drinking water supply, 4–9 million m^3/y for irrigation, 2 million m^3/y for industry and 2–3 million m^3/y for personal supply in 2010 (Sassine et al., 2015). This resource supports the economic activity surrounding Nîmes Metropolis. The shallow alluvial aquifer is composed of sands, gravel, and pebbles in a sandy-carbonated matrix, deposited by the paleo-Rhône River during the Plio-Quaternary period (Villafranchian, 3.5–1.0 Ma). Its thickness ranges from 10 to 15 m in the upgradient part to 30 m in the downgradient part, Poul et al. (1975).

The Garrigue area, made of lower Cretaceous limestones (136–130 Ma), borders the Vistrenque aquifer on its NW limit (Fig. 1C). The limestones were fractured and folded during the Pyrenean orogeny (Séranne et al., 1995; Benedicto et al., 1996). During the Oligocene, the Nîmes Fault acted as a normal listric fault and created a NE-SW trending basin. The Vistrenque hemi-graben was filled with syn-rift Oligocene-Aquitanian and post-rift Miocene sediments. Miocene Burdigalian outcrops can occasionally be found adjacent to Garrigues limestones. During the Lower Pliocene transgression, a thick layer of Plaisancian marine clays and marls were deposited (>300 m). These sediments correspond to the substratum of the Vistrenque aquifer. Above the lower pliocene sediments were deposited the villafranchian alluvial sediments by anastomosed rivers linked to the paleo-Rhône alluvial plain (Pantel, 2000). Quaternary deposits made of loess, silt, and recent alluvial sediments locally confine the Villafranchian aquifer.

2.2. Local hydrogeology of the study site

The sampling site is located in the upstream part of the Vistrenque aquifer (Fig. 1A). The average precipitation in this area is about 700 mm/year (http://pub-litheque.meteo.fr/) at the weather station of Nîmes Courbessac (10 km from the study site). The area is subject to a Mediterranean climate, with most of the precipitations occurring between autumn and winter. The recharge of the groundwater primarily occurs through precipitation where the aquifer is unconfined. With 25–30 % of effective rainfall, the annual recharge rate may be estimated between 180 and 220 mm (Pantel, 2009).

The main aquifer formation studied is the Villafranchian alluvial sediments. This aquifer has a transitivity ranging from 1.10^{-2} m^2/s to 1.10^{-4} m^2/s (Poul et al., 1975; Pantel, 2009). A second karstic aquifer,

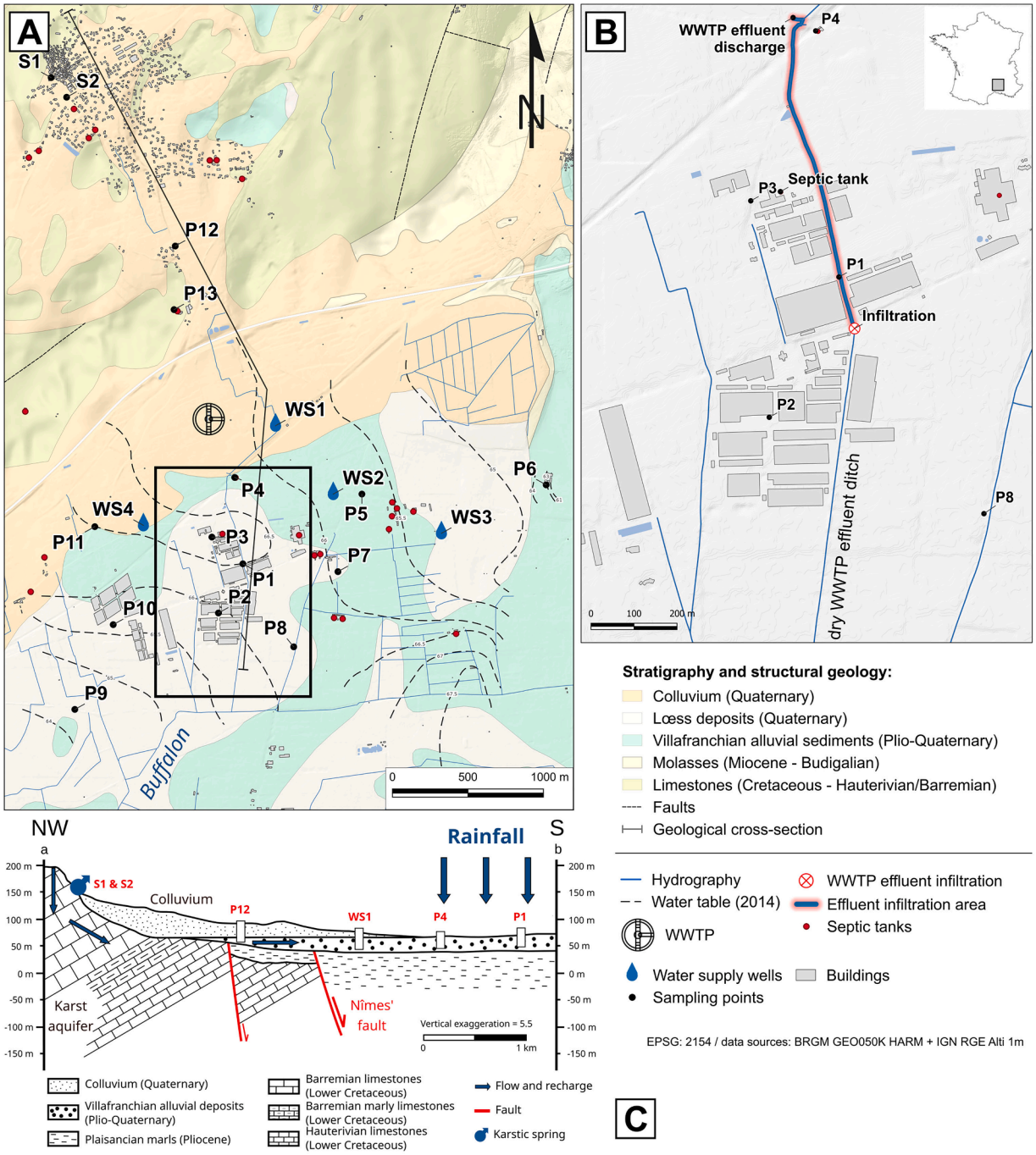

Fig. 1. [A] Hydrogeological map of the study area (water table data from HYDRIAD, 2015. WS1 to WS4 are the Water Supply wells, P1 to P13 corresponds to the groundwater samples, and S1 and S2 are karstic springs, [B] Focus on the centre of the study area (agro-industrial site) near the infiltration point of the WWTP effluent, [C] Geological cross-section from the Garrigues to the Villafranchian aquifer.

made of massive Hauterivian and Barremian limestones, outcrops in the northern part of the area (Garrigue). At the Garrigue's border, the Villafranchian alluvial sediments are covered by colluvium and the aquifer becomes semi-captive (Fig. 1C). The marked topography also shows an NNW-SSE incision of the limestones, corresponding to the filling of a paleo-valley by Quaternary sediments. Lateral recharge of the Villafranchian aquifer by the Cretaceous limestones was identified in previous studies (Ménillet and Palloc, 1973; Carbon et al., 2005).

In the study site, the thickness of the unsaturated zone varies between 3 and 8 m. According to the piezometric map, a localized high water table is visible at the centre of the area (HYDRIAD, 2015). From there, the groundwater flow is divided into 2 directions: the main one corresponds to the regional flow of the aquifer with a NE-SW direction, and the second one has a NW-SE direction, toward the eastern boundary of the Vistrenque aquifer (Fig. 1A).

2.3. Hydrography

The study area presents multiple small streams and ditches that drain water from the agricultural fields. These channels are mostly dry during summer. One of the ditches is fed by treated WWTP effluent, discharged into the environment (Fig. 1B). This ditch flows southward and merges

with the Buffalon River, located 2 km south of the effluent discharge point. During the dry season and periods of low rainfall, the effluent does not reach the river but instead infiltrates into the soil, approximately 600 m after the discharge point. This location is labelled as the "Infiltration" point on Fig. 1B. Hence, 100 % of the effluent is infiltrated where the aquifer is unconfined. The infiltration point is identified at the place where an ancient Roman aqueduct buried in the ground crosses the effluent ditch at the centre of the study area (Carbon et al., 2005). A small subsidence is observed directly above the buried aqueduct and can correspond to a preferential infiltration zone.

2.4. Land cover

The Vistrenque Plain is predominantly covered by agricultural activities, which represents 65 % of the land use at the study site (CORINE Land Cover, 2018). Approximately 50 % of the agricultural lands are dedicated to vineyards, while the remaining half consists of arboriculture, market gardening, cereal growing, olive groves and pastures with livestock. In addition to traditional agriculture, an agro-industrial site (vegetable seed producer for professionals) is situated in the centre of the study site. As there is no intensive livestock farming in the study area, there is no potential overlap of urban contaminants by veterinary pharmaceuticals.

Regarding urban contaminant sources, a WWTP is located in the centre of the study site. The station has a treatment capacity of 1500 population equivalent. The average daily effluent discharge between 2011 and 2021 was 150 m^3/d. The discharged effluent flows towards the Buffalon River (Fig. 1A), where pharmaceutical residues were detected in high concentrations (e.g., 304 ng/L^{-1} of diclofenac) in previous studies (Sassine, 2014, pp. 92).

In addition to the WWTP, there are dispersed septic tanks throughout the study area, which could also be point sources of emerging contaminants. Individual septic tanks are located near boreholes P3, P4, P7 and P13 (Fig. 1A). In addition, 6 septic tanks are found in a locality between P5 and WS3. Assuming that around thirty people are connected to these septic tanks, this represents 150 litres per day per points, spread over 3 km^2.

3. Material and methods

3.1. Sampling strategy

Groundwater sampling campaigns were divided into two periods, the dry and wet seasons, following the hydrological cycle. The first campaign was conducted between May and July 2021, and the second one took place between September and November 2022. In total, 4 drinking water supply wells (WS1 to 4), 11 piezometers in Villafranchian aquifer (P1 to P11), 2 piezometers in karstic aquifer (P12 and P13) and 2 karstic springs (S1 & S2) were sampled. The selection of sampling points was based on their relative position to the discharge area of the WWTP effluent (Fig. 1A and B).

Groundwater samples were collected using a submersible 2″ pump Grundfos MP1 when the piezometers were not already equipped. Each well was purged of at least 3 volumes of the water column until physicochemical parameters stabilized. Physicochemical parameters (temperature, electrical conductivity at 25 °C, pH and oxidation–reduction potential) were measured continuously in situ using a WTW 3630 multiparameter in a flow-through cell to prevent contact with the atmosphere.

Alkalinity was determined in the field as $CaCO_3$ (mg/L^{-1}) using a HACH® SL1000 Portable Parallel Analyser (PPA), equipped with low or high-range total alkalinity chemkey reagents. Based on the pH conditions, alkalinity was converted to HCO_3^- concentrations.

Samples of the WWTP effluent were collected during the summer of 2021 and the winter of 2022. A composite sample of the WWTP effluent was produced in November 2022 from 7 consecutive daily samples taken at different times of the day to account for the weekly variability of the effluent discharge.

Analysis of major and minor ions was carried out for both the 2021 and 2022 sampling campaigns. The analyses of pharmaceutical compounds were conducted either during the 2021 campaign, the 2022 campaign, or across both campaigns. Boron, $\delta^{11}B$, and REE were analysed only for 2021, except for the composite WWTP effluent sample, which was analysed in 2022.

3.2. Analytical methods

3.2.1. Major and minor ions analysis

Water samples were collected using a 60 mL HENKE-JECT® syringe (rinsed 3 times with the sample) and filtered with CA 0.45 µm filters (Sodipro) into 2 × 60 mL HDPE bottles. The bottle for cation analysis was acidified at pH~3 with HNO_3 (Merck, Suprapur) directly in the field.

Major ions (Cl^-, Na^+, K^+, Mg^{2+}, Ca^{2+}, SO_4^{2-}), bromide (Br^-) and phosphate (PO_4^{3-}) ions concentrations were analysed at the University of Nîmes (CHROME laboratory, France) by ion chromatography (Metrohm 930 Compact IC Flex, anion column: Metrosep A Supp 5 - 250/4.0, cation column: Metrosep C 6 - A150/4.0), at 35 °C for anions and 30 °C for cations, at a flow rate of 0.7 mL/min for anions (eluent: sodium bicarbonate 3.2 mM + sodium carbonate 1.0 mM) and 0.9 mL/min for cations (eluent: nitric acid 1.7 mM + dipicolinic acid 1.7 mM). The repeatability of the measurements is 5 %.

3.2.2. Boron concentrations, $\delta^{11}B$ and REE

Samples were collected in 125 mL HDPE bottles, following the same field sampling method as described previously for cation analysis.

Boron and Rare Earth Elements (REE) concentrations were determined by Inductively coupled plasma mass spectrometry atomic emission spectroscopy (ICP-OES/AES JY2000) at the Institut de Physique du Globe de Paris (IPGP) and by ICP-MS (Agilent 7900) at the University of Nîmes. To compare the results of both instruments, 5 samples previously analysed at IPGP were also analysed in Nîmes, with agreement between the two measures of better than 8 %.

Boron was extracted from the samples by ion exchange chromatography and isotope ratios were measured by multi-collector-ICP-MS (MC-ICP-MS Neptune, Thermo Scientific) at IPGP, Paris, France, using a direct-injection nebulizer (d-DIHEN, Analab), following Louvat et al., 2019. In addition, the composite WWTP effluent sample was analysed, at Advanced Isotopic Analysis (AIA) in Pau, France. The values are expressed in $\delta^{11}B$ (‰), using Eq. (1), relative to the NBS951 boric acid standard, measured in-between each sample as sample-standard bracketing.

$$\delta^{11}B\ (‰) = \frac{\left(^{11}B/^{10}B\right)_{sample}}{\left(^{11}B/^{10}B\right)_{standard}} - 1 \times 10^3 \quad (1)$$

The measurement uncertainty ranges from 0.25 to 0.5 ‰ (2SD).

To assess potential anthropogenic influences, REE abundances were normalized against a reference standard. The reference material used here is the European Average Shale (EAS) which is recommended for the normalization of REE in environmental and biological samples from Europe (Bau et al., 2018). The expected result of this normalisation is a smoothed curve. If a specific element deviates from this curve, the anomaly can be quantified from the normalised concentration (REE_N) and the interpolated concentration (REE*) (Knappe et al., 2005; Bau et al., 2018).

The Gadolinium anomaly (Gd/Gd*) can then be interpolated from the shale-normalised concentrations using the Eq. (2) (Hissler et al., 2015; Louis et al., 2020; Trommetter et al., 2022).

$$Gd/Gd^{*} = \frac{Gd_N}{(0.4 \times Nd_N + 0.6 \times Dy_N)} \quad (2)$$

where Nd_N is the shale-normalized neodymium (Nd) concentration; Dy_N is the shale-normalized dysprosium (Dy) concentration.

3.2.3. Pharmaceutical compounds

A total of 53 pharmaceutical compounds, including 20 therapeutic categories such as antibiotics, antidepressants, or anticonvulsants, were analysed on groundwater samples and composite WWTP effluent (Fig. 3). A full list of the pharmaceutical compounds and their therapeutic categories is provided in Supplementary Materials.

Pharmaceutical compounds were analysed following the methods of Gros et al., 2008 and Sassine et al., 2017. Samples were collected in pre-cleaned amber glass bottles, with Teflon-lined caps, rinsed three times by the sample itself. Upon collection, bottles were stored at 4 °C before conditioning. In the laboratory, 1000 mL of each sample was spiked with appropriate analytical surrogates to a concentration of 50 ng/L^{-1}. The sample was then filtered with Durapore® 0.45 µm PVDF Membrane. Solid Phase Extraction was carried out through Oasis HLB 6 cc (500 mg) LP Extraction Cartridge using a vacuum Visi-Prep (Phenomenex) by the ''catch to elute'' method. SPE cartridges were rinsed with 5 mL of MeOH, then conditioned with 5 mL of Milli-Q Water. The sample was loaded at ~5 mL/min. Elution was performed with 3 × 3.5 mL of MeOH, collected in 12 mL glass tubes. The solvent was evaporated under a gentle nitrogen flux and heated at 40 °C in a sample concentrator (Techne). Extracts were reconstituted with 250 µL of Milli-Q-MeOH (95:5) solution spiked with internal standards at a concentration of 50 ppb.

Samples were analysed in triplicates by HPLC-MS/MS (valve unit: FCV-11AL, degassing unit: DGU-20A, liquid chromatography: LC-20AD−XR, autosampler: SIL-30AC, column oven: CTO-20A, Shimadzu LCMS-8040) equipped with a reverse-phase separation system (pre-column: Polar C18 −2.1 mm, column: Kinetex Polar C18, 100A, 100 × 2.1 mm −2.6 µm Kinetex), at 40 °C, with a flow rate of 0.3 mL/min on a 20 min gradient (aqueous phase A: EUP+ 0.1 % formic acid v/v - organic phase B: MeOH + 0.1 % formic acid v/v).

The limits of detection and quantification (LOD and LOQ) were defined as 3 and 10 times the instrument signal-noise ratio, respectively (ICH, 2005). Measurement uncertainty (2SD), LOD and LOQ are provided in Supplementary Materials.

Table 1
Physical and chemical parameters, major and minor elements concentrations.

		T (°C)	EC (µS/cm^{-1})	TDS (mg/L^{-1})	pH	Eh (mV)	Cl^- (mmol.L^{-1})	Br^- (µmol.L^{-1})	Br/Cl
Water supply									
WS1	2021	16.0	740	474	7.0	401	0.79	1.7	2.2
	2022	15.9	748	479	7.1	469	0.84	2.1	2.5
WS2	2021	16.0	796	509	7.1	437	0.85	3.6	4.3
	2022	16.4	795	509	7.0	419	0.8	2.3	2.8
WS3	2021	17.0	736	471	7.1	360	0.93	1.7	1.9
	2022	15.3	746	477	6.8	414	1.06	1.9	1.7
WS4	2021	15.5	713	456	7.0	423	0.56	1.2	2
	2022	16.6	739	473	7.1	461	0.64	1.4	2.1
Villafranchian aquifer									
P1	2021	16.7	1391	890	7.0	337	3.68	2.7	0.6
	2022	–	–	–	–	–	–	–	–
P2	2021	16.8	1100	704	7.1	389	1.99	2.2	1.1
	2022	–	–	–	–	–	–	–	–
P3	2021	17.0	1137	728	7.0	399	1.79	2.7	1.5
	2022	–	–	–	–	–	–	–	–
P4	2021	16.9	1214	778	7.0	317	2.9	2.2	1.3
	2022	16.4	1105	707	6.8	320	3.84	2.7	0.7
P5	2021	16.4	798	511	7.1	360	0.89	2.5	2.8
	2022	18.3	756	484	6.5	316	0.77	2.2	2.8
P6	2021	16.0	610	390	7.0	371	0.74	1.3	1.7
	2022	–	–	–	–	–	–	–	–
P7	2021	16.2	1088	696	6.9	302	1.36	1.7	1.2
	2022	–	–	–	–	–	–	–	–
P8	2021	15.2	643	412	7.1	452	0.45	1	2.2
	2022	15.8	659	422	6.5	344	0.47	1.2	2.5
P9	2021	16.3	987	632	7.1	314	1.45	2	1.3
	2022	16.8	800	512	6.9	274	1.3	2.4	1.9
P10	2021	15.8	703	450	7.3	385	0.85	1.6	1.9
	2022	19.1	792	507	6.9	295	1.05	2	1.9
P11	2021	16.5	762	488	7.0	352	0.62	1.3	2.2
	2022	17.0	742	475	6.6	321	0.64	1.6	2.4
Cretaceous karst aquifer									
P12	2021	16.0	862	552	6.9	324	0.52	0.9	1.7
	2022	–	–	–	–	–	–	–	–
P13	2021	16.5	959	614	6.8	418	1.16	17.4	15
	2022	–	–	–	–	–	–	–	–
S1	2021	12.8	921	589	6.9	336	0.28	0.8	3.1
	2022	13.0	740	474	7.2	361	0.36	0.5	1.5
S2	2021	13.3	891	570	6.8	365	0.3	1	3.2
	2022	17.2	554	355	7.4	419	0.33	0.7	2.2
Urban effluent									
WWTP effluent	2021	23.0	1533	981	7.7	–	6.03	2.4	0.4
	2022	10.3	1013	648	7.7	400	5.03	1.6	0.3
WWTP composite sample		11.2	1150	736	7.1	433	5.29	2.1	0.4
WWTP after storm		12.1	1176	753	6.9	294	3.16	1.1	0.3
Septic tank		11.6	1659	1062	7.7	238	3.33	2.8	0.9

4. Results

4.1. Physical & chemical parameters

Physical and chemical parameters measured in the field are presented in Table 1.

The electrical conductivity (EC) of groundwater varies significantly, ranging from 554 to 1391 µS/cm^{-1} (median = 792 µS/cm^{-1}). Based on previous studies, the average EC of the Villafranchian aquifer in this part of the Vistrenque basin is around 800 µS/cm^{-1} (Sassine et al., 2015). The effluent from the WWTP shows an EC of 1533 µS/cm^{-1} measured in summer and 1013 to 1176 µS/cm^{-1} in the 2 samples collected in winter. The winter sample with the lowest EC was measured after a heavy rainstorm. The septic tank effluent, located near the piezometer P3 and sampled in February 2022, displays the highest EC at 1659 µS/cm^{-1}.

4.2. Elemental tracers

Based on major ions' analysis, groundwater samples have bicarbonate calcium geochemical facies (Supplementary materials), whereas WWTP and septic tank effluent are sodium chloride type waters. Some groundwater samples tend toward the sodium chloride facies, such as P1 and P2.

On the Vistrenque plain, the chloride reference value "Cl_{ref}", corresponding to the natural chloride input from evapo-concentrated rainwater infiltration to groundwater, (Grosbois et al., 2000; Huang and Pang, 2011), varies between 0.05 and 1.1 mmol.L^{-1} (Ladouche et al., 2009; Sassine et al., 2015). Chloride concentration above the Cl_{ref} implies an additional source of Cl^- in the system.

In the study area, the Cl^- concentrations of the groundwater samples range from 0.36 to 3.8 mmol.L^{-1} (median = 0.85), which is up to 3.5 times the Cl_{ref}. Sampling points showing concentrations above the Cl_{ref} are P13, P9, P7, P2, P3, P1, P4, ranked with increasing Cl^- concentrations.

The average Cl^- concentration of urban effluents is 5.1 mmol.L^{-1}. Similarly to EC, Cl^- concentration of the WWTP effluent may drop just after a rain (here, by half during the sampling campaign).

The Br/Cl molar ratio (mmol/mmol ×1000) decreases with increasing Cl^- concentrations (Fig. 2). The Br/Cl_{molar} values of groundwater samples range from 0.57 to 4.24, while it is 1.57 for seawater (Cook and Herczeg, 2000). Point P13 has an anomalously high Br/Cl ratio of 15. The samples with the lowest ratios are P1, P2, P3, P4, P7 and P9. The urban effluent also shows a low Br/Cl_{molar} ratio of 0.34 on average, consistent with previous studies (Vengosh and Pankratov, 1998; Panno et al., 2006; Katz et al., 2011; McArthur et al., 2012).

Phosphates were measured in urban effluents, but their concentrations were below quantification limits in groundwater (Supplementary materials).

4.3. Organic tracers

Pharmaceutical compounds were detected in all groundwater samples, except P8 and P12. Caffeine (CAFE), lidocaine (LIDO), epoxycarbamazepine (ECBZ), fluconazole (FLUCO), carbamazepine (CBZ), sulfamethoxazole (SFMX), tramadol (TRA) and lamotrigine (LAMO) were detected in more than 50 % of the groundwater samples. The detection frequencies for each compound were as follows: CAFE (f = 91 %), LIDO (f = 82 %), ECBZ (f = 77 %), FLUCO (f = 77 %), CBZ (f = 73 %), SFMX (f = 73 %), TRA (f = 68 %), and LAMO (f = 55 %). Sample concentrations are presented in Fig. 3.

Here, the concentration of CBZ ranges from 0 to 532 ng/L^{-1} (mean: 98 ng/L^{-1} / median: 18 ng/L^{-1}) (Table 2). Sample P1, the closest to the WWTP effluent infiltration point, has the highest concentrations with a total concentration of pharmaceuticals of $\Sigma_{19\ detected\ PHARM}$ = 2027 ng/L^{-1}.

As expected, the composite WWTP effluent shows greater concentrations in pharmaceutical compounds compared to groundwater. FLUCO, CBZ, ECBZ, LIDO, and TRA were exceptions. However, some molecules were only found in the effluent and not in the groundwater, such as escitalopram, ciprofloxacin, verapamil, amitriptyline, ofloxacin, trimethoprim, fluoxetine, diphenhydramine, mefenamic acid, atenolol, erythromycin, spiramycin and warfarin.

4.4. Boron isotopes and concentrations

The boron concentrations of groundwater samples have an average value of 57 µg.L^{-1}, with a maximum concentration of 152 µg.L^{-1} at the piezometer P4. Boron isotopic signature $\delta^{11}B$ varies significantly from

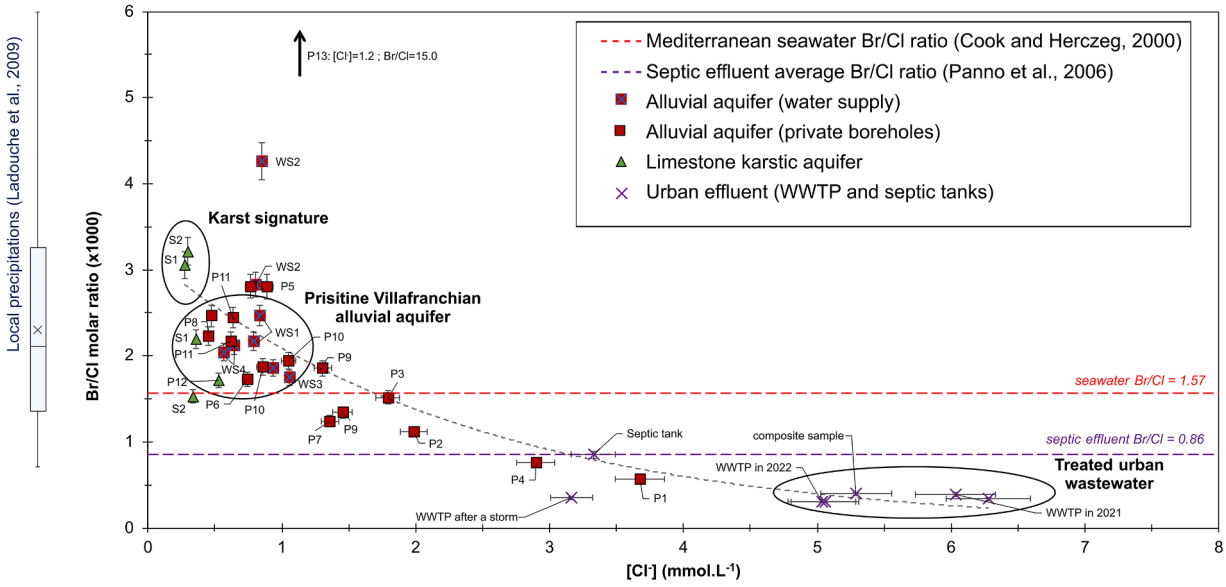

Fig. 2. Plot of the Br/Cl ratio (×1000) versus chloride concentrations (mmol L^{-1}) from groundwater and urban wastewater samples (err. 5 %). Br/Cl ratios of local precipitations derived from Ladouche et al. (2009).

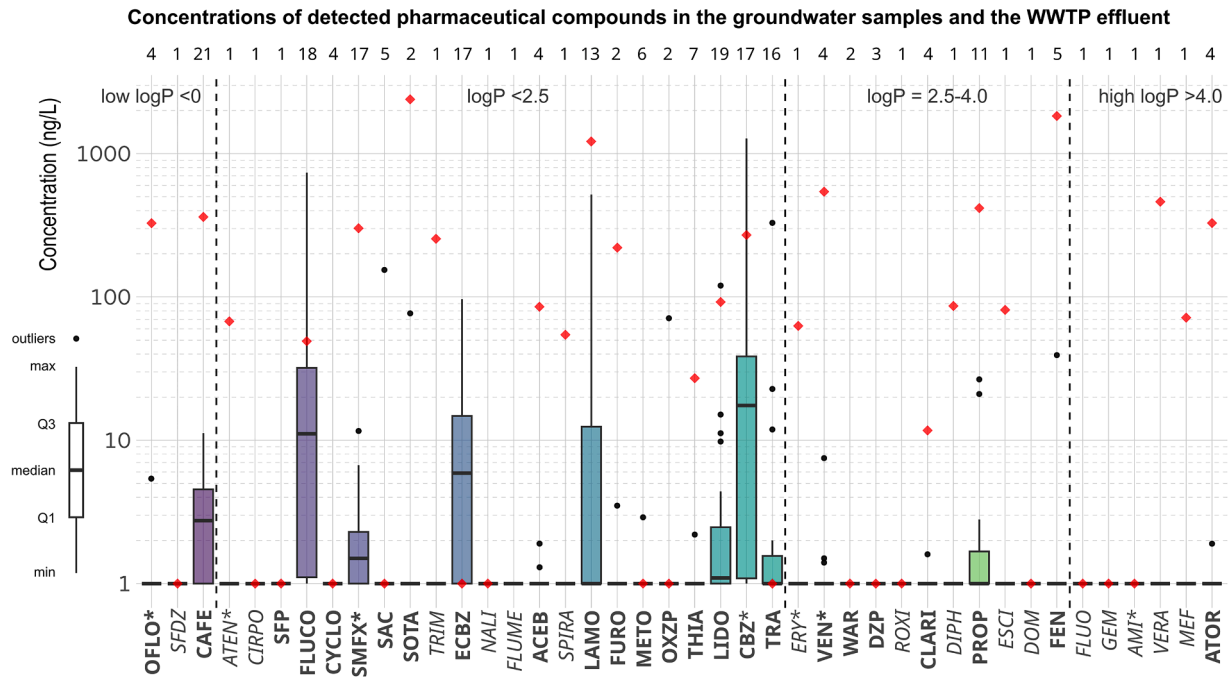

Fig. 3. Concentrations of detected pharmaceutical compounds in groundwater samples (boxplots) and WWTP effluent (red diamonds), classified according to their partition coefficient (logP). The numbers of detections in the groundwater and the effluent are indicated at the top of the graph. Pharmaceutical compounds written in bold are found in groundwater, those written in italic are only detected in the WWTP effluent, and those identified with "*" have a corresponding internal standard (ISTD). The full list of abbreviations is available in Supplementary Materials.

Table 2
Data for organic tracers (carbamazepine (CBZ) and epoxy-carbamazepine (ECBZ)), REE (neodymium, gadolinium, dysprosium), gadolinium anomaly (Gd/Gd*), boron concentrations and $\delta^{11}B$. Samples were analysed in 2021, except for the WWTP composite sample analysed in 2022. "ND" not detected, "MQL" method quantification limit, "–" not analysed.

	CBZ (ng/L^{-1})	ECBZ	Nd (ng/L^{-1})	Gd	Dy	Gd/Gd*	B ($\mu g.L^{-1}$)	B RSD (%)	$\delta^{11}B$ (‰ vs. NBS951)	2SD $\delta^{11}B$ (%)
Water supply										
WS1	17.8	ND	3.4	3.3	1.1	3.5	67.2	4.7	22.02	0.25
WS2	36.4	15.0	5.4	9.5	1.2	8.6	49.9	1.6	23.93	0.25
WS3	14.0	7.9	25.6	11.9	4.5	2.6	48.4	2.5	28.24	0.25
WS4	ND	ND	4.7	1.2	1.4	1.0	25.1	2.1	23.81	0.25
Villafranchian aquifer										
P1	420.0	34.6	0.6	535.1	0.9	871.9	140.1	1.9	7.73	0.25
P2	242.1	21.9	0.2	67.6	0.2	432.8	109.2	2.6	11.38	0.25
P3	22.7	<MQL	2.0	26.7	0.8	41.3	46.2	2.6	27.90	0.25
P4	532.1	39.4	<MQL	84.0	<MQL	–	152.2	2.3	4.65	0.25
P5	38.1	8.4	17.1	12.3	3.2	3.8	48.3	1.5	25.21	0.25
P6	–	–	18.6	5.1	3.8	1.4	26.9	3.4	18.62	0.25
P7	–	–	14.1	13.0	3.5	4.1	42.8	4.7	33.57	0.25
P8	ND	ND	12.7	2.5	4.0	0.7	20.6	1.7	33.42	0.25
P9	24.4	<MQL	7.1	8.8	2.0	5	28.1	2.7	24.25	0.25
P10	9.9	13.0	6.6	7.0	1.8	4.4	18.6	4.5	26.46	0.25
P11	ND	ND	4.5	2.4	1.3	2.1	27.3	2.8	18.9	0.25
Cretaceous karst aquifer										
P12	ND	ND	<MQL	0.47	<MQL	–	31.0	2.0	19.47	0.25
P13	ND	ND	3.6	6.6	0.9	8.2	86.5	3.4	19.14	0.25
Urban effluent										
WWTP effluent (2021)	525.6	106.5	–	–	–	–	–	–	–	–
WWTP composite sample	264.9	75.2	–	–	–	–	124.5	4.6	9.44	0.41

4.7 to 33.6 ‰ (median = 23.8 ‰). The three most B concentrated samples (points P2, P1 and P4, respectively, with increasing boron concentrations) are also the ones with the lowest isotopic signatures (Fig. 4A). These samples are located near the infiltration point and close to a septic tank (Fig. 1B).

The WWTP effluent composite sample has a boron concentration of 125 $\mu g.L^{-1}$ and a $\delta^{11}B$ isotopic signature of 9.4 ‰. This value is consistent with those found in other studies (Vengosh et al., 1994; Seiler, 2005; Chalk, 2020).

4.5. Gadolinium

The gadolinium anomaly Gd/Gd* in groundwater ranges from 0.7 for P8 up to 872 for P1(median value of 4.2). Gd anomalies above 1.4–1.8 indicate an anthropogenic input of Gd to the groundwater system (Rabiet et al., 2009; Louis et al., 2020). In the present study, P6, P8

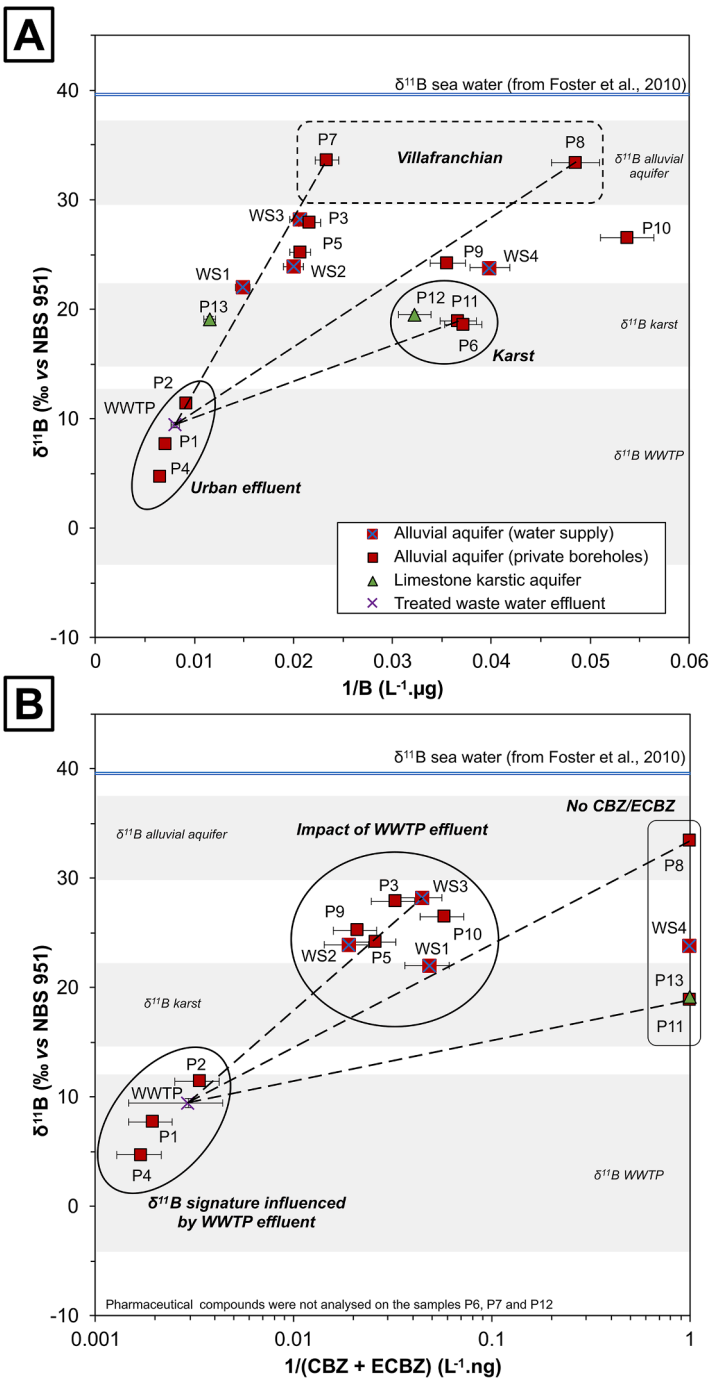

Fig. 4. [A] Variations of boron isotopic signatures $\delta^{11}B$ (‰ vs. NBS951) and 1/B concentrations (L/µg) [B] Comparison of boron isotopic signatures $\delta^{11}B$ (‰ vs. NBS951) and 1/(carbamazepine + epoxy-carbamazepine) concentrations (L/ng) for groundwater and urban effluents samples. Boron isotopic signatures for WWTP from Chalk, 2020.

and WS4 show Gd/Gd* values below 1.4 and do not seem to be impacted by the WWTP effluent based on the piezometric data (Fig. 1A). The highest Gd/Gd* values are observed for all the groundwater samples located at the centre of the study area (Fig. 5B), while the samples most distant from the infiltration point show lower ratios.

As Nd and Dy concentrations in P4 and P12 were below the analytical quantification limits (Table 2), the Gd/Gd* values for these samples are over-estimated. The Gd/Gd* measurement can be problematic if one of the elements used for the interpolation is anomalous itself (Bau and Dulski, 1996; Lawrence and Kamber, 2006; Kulaksız and Bau, 2011). Therefore, P4 and P12 were not included in the discussion about Gd/Gd*.

The composite WWTP effluent sample was only analysed for Gd concentration, therefore no Gd/Gd* anomaly could be calculated for this sample.

5. Discussion

5.1. Identification of a WWTP effluent plume

5.1.1. Geochemical evidence for the WWTP effluent infiltration into the aquifer

Samples collected near the assumed infiltration point show a relatively high EC compared to EC of groundwater in the same formation

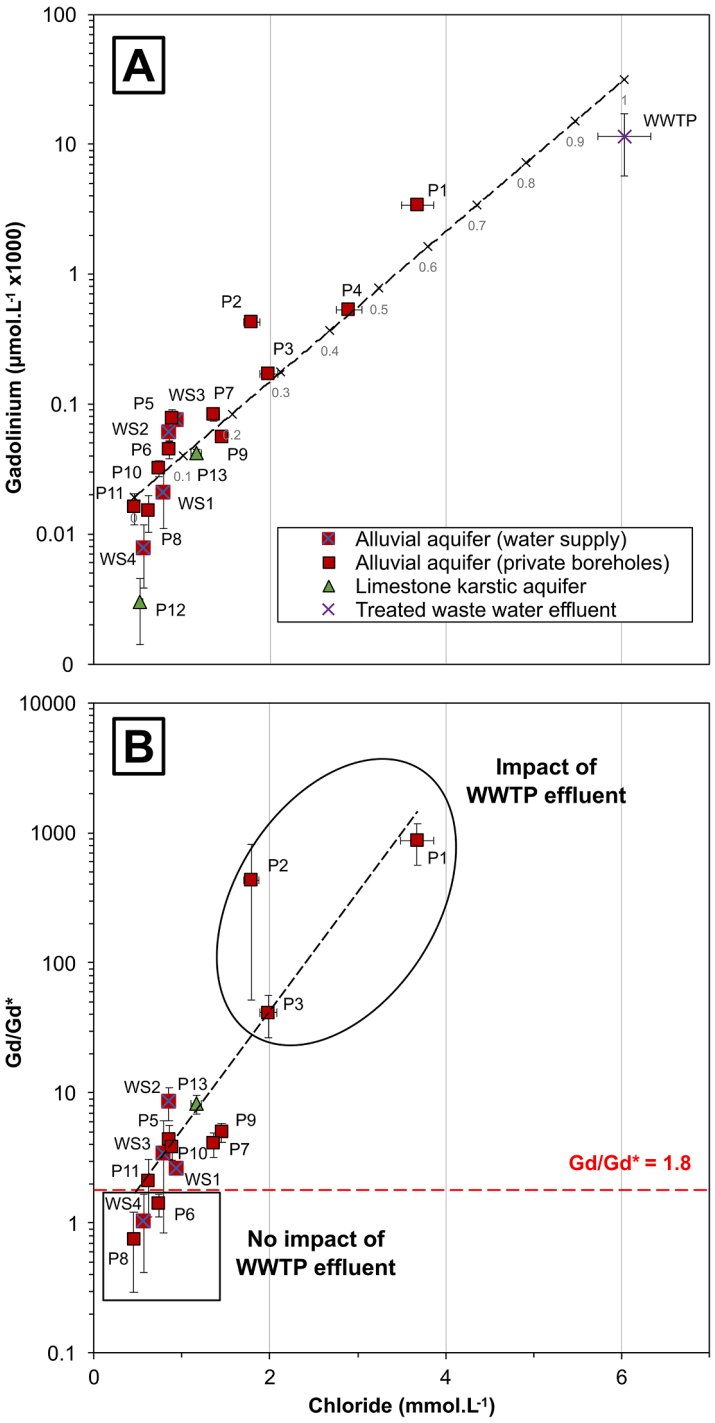

Fig. 5. [A] Correlation between gadolinium and chloride concentrations and derived mixing fractions, [B] Gd/Gd* anomaly for groundwater samples. P4 and the WWTP effluent are not included.

and at the same depth. These samples are marked by high Cl^- concentrations above the Cl_{ref} of 1.1 mmol.L^{-1} (Table 1).

From the Br/Cl molar ratio vs. chloride concentration diagram (Fig. 2), an average Br/Cl ratio of 1.90 for the non-impacted Villafranchian groundwater can be defined, consistent with the Br/Cl ratio of rainwater in the south of France and its seasonal variations (Ladouche et al., 2009). The karst Br/Cl is similar to the Villafranchian ratios and fits also within the range of the regional rainwater Br/Cl variations. The samples WS2 of 2021 and P13 have a higher Br/Cl ratio than the other groundwater samples. This could indicate another source of Br, such as anthropogenic contribution of particulate matter and halogens to the atmosphere, or the use of Br-based fertilizers (Alcalá and Custodio, 2008). The Br/Cl increase could also be attributed to the release of gaseous bromide in the atmosphere, linked to forest-burning during summer (Ladouche et al., 2009). Sample P13 is located less than 10 m from a private swimming pool. Depending on the disinfection type (chlorinated or brominated), swimming pools emptying could be a local source of Br within the aquifer, as brominated swimming pool waters should have higher Br/Cl ratios (Richardson et al., 2010).

The treated urban effluent seems to form a coherent endmember, with a depleted Br/Cl ratio of 0.34 and high chloride concentration. The Br/Cl molar ratios of the groundwater samples suggest a mixing trend

between the non-impacted Villafranchian groundwater and urban effluents. This suggests an infiltration of the WWTP effluent into the aquifer, with a sufficiently large volume to impact the groundwater chemistry. Samples below the seawater Br/Cl ratio (1.57) can be considered as impacted by the WWTP effluent, as no other source of depleted Br/Cl ratio has been identified in the area.

Considering an average Br/Cl ratio of 1.90 for the non-impacted Villafranchian aquifer and a Br/Cl ratio of 0.34 for the WWTP effluent, the proportion of effluent in the mix can be calculated (Vengosh and Pankratov, 1998). For the samples P1, P2, P3 and P4, the urban endmember contributes to respectively 67 %, 32 %, 14 % and 58 % of the water. Sample P1, closest to the supposed infiltration zone, has the highest contribution of WWTP effluent. As expected, the urban effluent fraction decreases with increasing distance from the infiltration point towards P2. This observation appears to be consistent with the piezometric map showing a main groundwater flow direction towards the SE (Figs. 1A and 6). The increase in WWTP effluent contribution at P4 suggests a second groundwater flow direction, towards the NW.

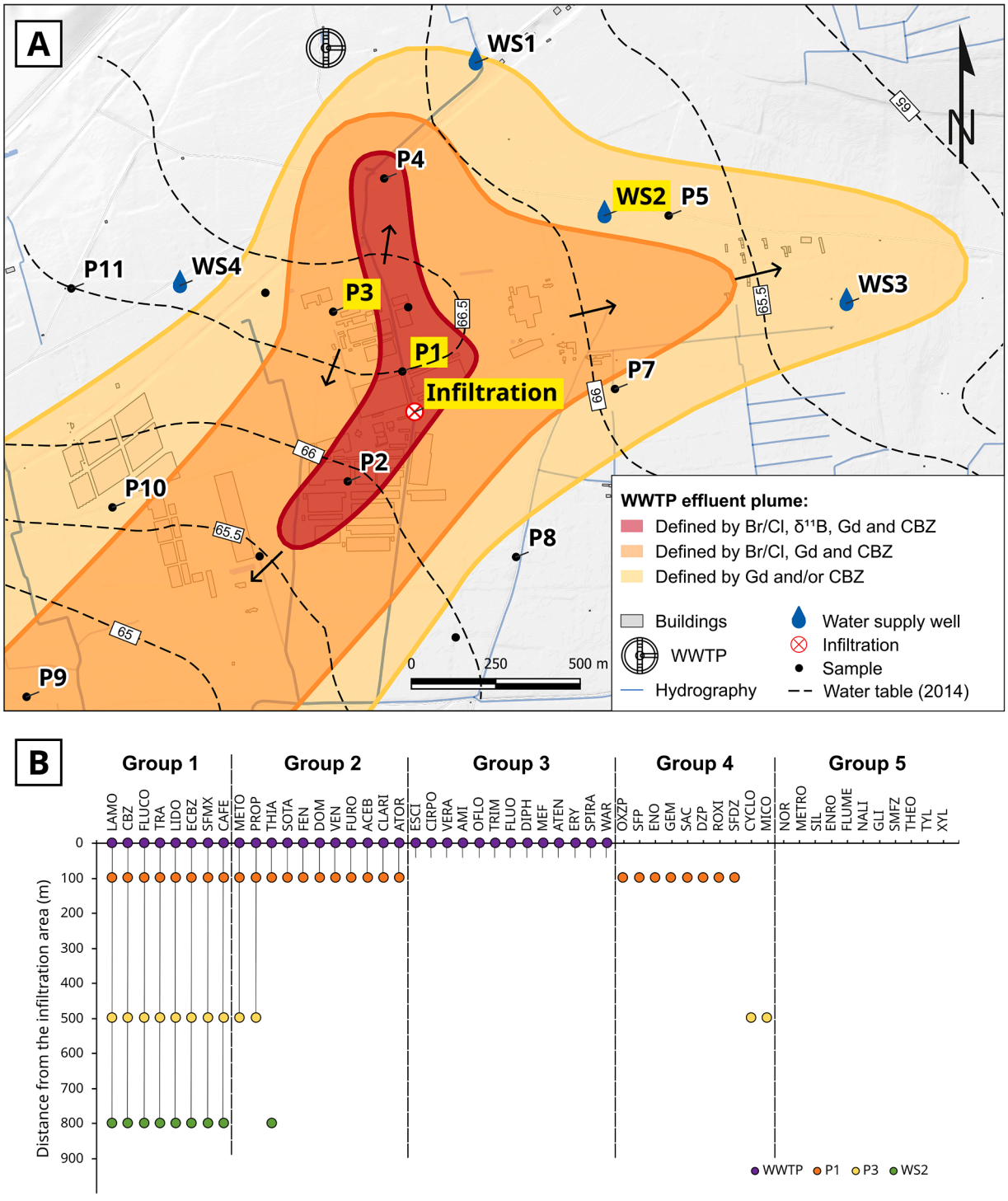

Fig. 6. [A] Plume spatial extent based on the multi-tracer approach. The areas depend on the number of tracers which were used to detect the WWTP effluent plume [B] Evolution of the detected pharmaceutical compounds along the plume transect. Selected samples are highlighted on the map.

Although P3 is close to the infiltration point, it is not located within the main groundwater flow, and therefore less influenced by the WWTP effluent. The contaminant transport and the shape of the plume seems to be related to the water table high identified on the piezometric maps.

5.1.2. Use and limitation of boron isotopes

While the study area is only 7 km^2, the $\delta^{11}B$ isotopic signature of groundwater samples highlights a significant variability. The local karst aquifer isotopic signature at 19.0 ‰ can be defined from the samples P11, P12 and P13 (Fig. 4), in good agreement with the carbonate $\delta^{11}B$ endmember defined in another study of groundwaters in SW France (Négrel et al., 2012). Sample P8, located at the southern border of the area, hence disconnected from the karst aquifer, represents the Villafranchian endmember with a $\delta^{11}B$ of 33.4 ‰. More important rainfall contribution could explain the higher $\delta^{11}B$ signature of the Villafranchian, as coastal precipitations $\delta^{11}B$ signature is influenced by seawater (Millot et al., 2010). Most of the samples show an isotopic signature comprised between the karst and Villafranchian signatures (19 ‰ and 33.4 ‰), suggesting that the alluvial aquifer waters are naturally influenced by lateral recharge from the karst aquifer. However, samples P3, P5, P7, WS1, WS2 and WS3 have slightly higher boron concentrations than P8. This may suggest another source of boron, linked to the use of fertilizers (Widory et al., 2005), or a mixing with an enriched source of boron, such as urban effluents (Cary et al., 2013).

Some of the groundwater samples, such as P1 and P4, have a slightly lower $\delta^{11}B$ isotopic signatures compared to the WWTP and are identified as impacted by the WWTP effluent with the Br/Cl ratio. This may suggest a variability in the isotopic signature of the effluent depending on the amount and origin of B-containing products (Guinoiseau et al., 2018), or a dilution of the WWTP $\delta^{11}B$ signature by rainwaters during rainy periods. Downstream of the WWTP outlet, low $\delta^{11}B$ signatures indicate a clear impact of WWTP effluent for P1, P2 and P4. Although P3, P7 and P9 do not have a significantly low $\delta^{11}B$ signature, they plot on mixing trend between pristine groundwater and the urban effluent end member on the Br/Cl plot. This suggests two mixing lines on the 1/B-$\delta^{11}B$ plot (Fig. 4A): the first one, from P7 to the WWTP effluent, and the second one from P8 and the WWTP effluent. Based on these mixing lines, WS1, WS2, WS3 and P5 could be impacted by the WWTP effluent.

The impact of the urban effluent end member on the boron isotopic signature appears to diminish rapidly as the distance from the infiltration point increases. Only P1, P2 and P4 show a clear impact of the WWTP effluent. This could be due to the gradual dilution of the plume of contaminants with the groundwaters, in the absence of a real contrast in B concentration between pristine groundwaters and WWTP effluents (only 5 times more B concentrated in average). Boron concentrations may suggest that P5, WS1, WS2 and WS3 are impacted by WWTP effluent, but more evidence is needed to confirm this observation. In this case study, while $\delta^{11}B$ clearly highlights the occurrence of a WWTP plume, it does not seem sensitive enough on its own to delimit the plume extent.

5.1.3. Combination with organic tracers

Within the most detected pharmaceutical compounds in groundwater (i.e., CAFE, LIDO, CBZ, ECBZ, FLUCO, SFMX, TRA and LAMO), CBZ and its metabolite ECBZ, are very persistent in the environment, thus being good tracers of anthropogenic sources (Clara et al., 2004). CBZ+ECBZ concentrations and $\delta^{11}B$ are presented in Fig. 4B. P1 and P2, samples closest to the infiltration point, have the lowest $\delta^{11}B$ signatures and the highest concentrations of CBZ+ECBZ, pinpointing the impact of the WWTP effluent. Although WS1, WS2, WS3, P3, P5, P9, and P10 do not have particularly low $\delta^{11}B$ signatures, the presence of significant carbamazepine concentrations (i.e., ~30 ng/L^{-1}) highlights the influence of the urban end member on these samples. Note that the lack of sensitivity of $\delta^{11}B$ alone in tracing the extent of the plume is linked to the low variability of B concentrations, over barely one order of magnitude, whereas CBZ+ECBZ concentrations vary over 3 orders of magnitude (Fig. 4A and B). While WS1, WS2 and WS3 were not considered as impacted by the effluent on the Br/Cl model, the presence of pharmaceutical compounds clearly highlight the extent of the plume to these points. P4 also has higher concentrations of CBZ compared to other groundwater samples located closer to the infiltration area, such as P1, and have higher total CECs concentrations than the observed WWTP effluent itself. These observations, combined with the boron concentrations, suggests either a variability in the B and CBZ concentrations of the WWTP effluent, or a local source of contaminants such as septic tanks. Indeed, sample P4 is a borehole in a private property that has on-site sanitation in the directed vicinity (<10 m) of the borehole, which could be a point source for pharmaceutical compounds in this section of the aquifer. Due to accessibility constraints, this septic tank effluent could not be sampled. Nevertheless, the discharge rate of a single septic tank is negligible with respect to that of the WWTP at the global scale, but its impact on the groundwater could nonetheless be detected locally with the CECs.

5.2.4. Gadolinium as a conservative tracer

All samples showing Br/Cl, $\delta^{11}B$ or CBZ+ECBZ contamination have Gd/Gd* values higher than 1.8, indicating mixing with WWTP effluent. By coupling Gd and Cl^- concentrations, a mixing trend can be observed between the WWTP effluent and the non-impacted alluvial endmembers (Fig. 5). This mixing trend suggests that Gd has a conservative behaviour in the aquifer. It should be noted that P4 is aligned with the mixing trend between the non-impacted alluvial endmember and the WWTP effluent.

Overall, $\delta^{11}B$, Gd and CBZ are complementary to assess the spatial extent of the WWTP plume. Gd and Gd/Gd* show a large range of concentrations and can be considered as a reliable tracer of WWTP effluent. Based on the Cl-Gd relationship, the contributions of the WWTP effluent for P1, P2, P3 and P4 are respectively: 70 %, 42 %, 29 % and 45 %. These results are similar to those obtained with the Br/Cl ratio.

5.3. Critical assessment of the different tracers

Based on the Br/Cl ratio alone, an influence of urban effluent infiltration in groundwater is observed. P1, the closest to the infiltration point, is the most impacted by the WWTP effluent signature, followed by P4, P3 and P2. While efficient, this tracer alone does not have sufficient resolution to highlight impacted wells with a Br/Cl value above 1.5 (Fig. 2).

Although phosphates can be a tracer of urban effluents (Huang et al., 2020), the absence of significant concentrations in groundwater makes them unsuitable for this study area.

The boron concentrations and isotopic signatures provide complementary information to the Br/Cl ratio. They confirm the occurrence of WWTP effluent mixing within the aquifer. However, this tracer also does not have sufficient resolution to delimit the extent of the plume, due to the lack of real contrast in the context of this study between the B concentrations of WWTP effluent and of the non-impacted alluvial aquifer. Only points closest to the infiltration point show a signature towards the WWTP endmember. Locally, boron concentrations and $\delta^{11}B$ can be modified. The proximity of the P4 with a septic tank could be the reason for the slightly higher boron concentrations and a lower $\delta^{11}B$ signature. Without further data, $\delta^{11}B$ alone cannot be used to characterize the plume. In particular, the variability of the $\delta^{11}B$ signature of the WWTPs should be considered (Vengosh et al., 1994; Seiler, 2005), and the fact that this signature can change through time (Guinoiseau et al., 2018), depending on the anthropic B sources and uses.

The pharmaceutical tracers, in particular CBZ and ECBZ, seem more reliable for assessing the plume extent. By pairing CBZ concentration and $\delta^{11}B$, it is now possible to identify impacted samples which had not been identified as being impacted by the WWTP effluent with the Br/Cl. Nevertheless, the use of pharmaceutical tracers also has limits. Although patients taking CBZ are prescribed a daily dose, and it is a persistent molecule, average effluent concentrations may have inter-annual

variability. Pharmaceutical tracers are also sensitive to point source contamination, such as septic tanks, both of which must be taken into account during the interpretation.

In the study area, the origin of excess Gd is due to WWTP effluent. Although septic tanks can have a local influence on groundwater (e.g. sample P4), gadolinium can be used to minimise these sources of local contamination when delimiting the WWTP plume. Pairing the Gd, Gd/Gd* and Cl^- concentrations shows that Gd could be used as a conservative tracer for assessing plume extent in groundwater. Gd needs to be paired with other tracers, according to the local hydrogeological context, to provide better evidence of mixing processes. The origin of Gd in WWTP is linked to the presence of magnetic resonance imaging facilities, which are not present in every urban area, limiting its use as tracer of anthropogenic effluents for small towns and villages.

Each of the tracers used in this study has its specificities and limitations, as they indicate different types of anthropic effluents to the groundwaters, but their combination efficiently increases the resolution of the anthropogenic plume impact and extend as well as its origins.

The WWTP plume shape and extent have been defined based on the multi-tracer approach (Fig. 6A). Here, the following criteria for water being impacted by WWTP effluent were used: Br/Cl < 1.6, $\delta^{11}B < 12$ ‰, detection of carbamazepine, and Gd/Gd* > 1.8. Samples P1, P2 and P4 meet all the criteria, while $\delta^{11}B$ did not reveal the plume signature on P3 and P9. Finally, WS1, WS2, WS3, P5 and P10 were considered part of the plume based on organic tracers only. Thus, the shape and extent of the plume was more precisely defined when all tracers were combined. The WWTP plume shape is consistent with the piezometry (Figs. 1A and 6), following the main NE-SW flow. A second direction, with an E-W orientation, extends towards WS2 and WS3. From WS3 to P9, the plume is 3 km long, and appears to extend outside the study area towards the SW.

5.4. Degradation of the pharmaceutical compounds along the plume

The occurrence of pharmaceutical compounds along the plume also provides information on their degradation in the environment. Several mechanisms can affect pharmaceutical residues during their travel time in surface water or their transfer through the unsaturated zone. These processes include sorption (and desorption) on organic or mineral particulate phases, hydrolysis, biodegradation, and UV photodegradation (only in surface water) (Khan et al., 2020; Bavumiragira et al., 2022). Depending on the intensity of these processes and their properties, pharmaceutical compounds can be mineralized, partially degraded, or not degraded at all. The presence or absence of pharmaceutical compounds was compared to the WWTP effluent, P1, P3 and WS2 samples (Fig. 6B). These samples are considered to be representative of the evolution of the plume with distance from the infiltration point.

Based on this approach, five groups of pharmaceutical compounds were defined:

- Group 1 are compounds detected in both the effluent and all 3 selected groundwater samples. It includes carbamazepine, epoxycarbamazepine, caffeine, lamotrigine, fluconazole, tramadol, lidocaine, and sulfamethoxazole. Most of these compounds were already reported in previous studies as potential tracers for the evaluation of wastewater impact on groundwater (Cary et al., 2013; McCance et al., 2018, 2020).
- Group 2 are compounds detected in the effluent and P1. This group includes metoprolol, propanolol, thiabendazole, sotalol, fenofibric acid, domperidone, venlafaxine, furosemide, acebutolol, sulfapyridine, clarithromycin and atorvastatin. These compounds are only found close to the infiltration area, suggesting rapid attenuation within the soil/aquifer system.
- Group 3 are compounds only detected in the WWTP effluent and are not found in groundwater. These compounds show a total attenuation in their migration through the unsaturated zone, suggesting mechanisms such as sorption or biodegradation (Kodešová et al., 2016; Gworek et al., 2021).
- Group 4 are compounds detected in groundwater samples close to the infiltration area, but not detected in the WWTP effluent. This could be due to variable concentrations of these pharmaceutical compounds in the effluent, that could for example be due to a variable number of people under treatment, with a delayed environmental remanence. Note that WWTP effluents and groundwaters were not sampled at the same date.
- Group 5 are compounds that were not detected in this study, in either the effluent or groundwater. These compounds may be absent from the WWTP influent or be degraded by the WWTP.

By highlighting these groups, emphasis can be placed on group 1 and 2 for the use of pharmaceutical compounds as co-tracers to delineate WWTP plume, in addition to conventional geochemical and isotopic tracers.

6. Conclusion

The present multi-tracer approach based on geochemical, isotopic, and organic data appears to be a reliable method to study the infiltration of WWTP effluent in groundwater.

Conventional analyses such as electrical conductivity, chloride concentrations and Br/Cl ratio are sufficient to detect the presence of a plume due to the strong urban influence near the infiltration point. However, these tracers become less efficient as the plume fades away with increasing distance from the infiltration point. This limitation can be overcome by using complementary tracers such as $\delta^{11}B$, contaminants of emerging concern (CECs) such as carbamazepine (CBZ), or REE such as gadolinium (Gd).

In the study area, the influence of the plume is still visible up to 1.5 km downstream, both in Gd and CBZ concentrations. By coupling $\delta^{11}B$ and CBZ, some samples that were not detected with conventional tracers are revealed to be impacted by the WWTP plume. Among these points are two drinking water supply wells, both showing signs of contamination. However, pharmaceutical compounds concentrations may be impacted by degradation or by mixing with point-source contamination, such as septic tanks. Organic tracers are also unreliable on their own and should therefore be combined with geochemical or isotopic tracers.

Gadolinium proved to be a conservative and reliable tracer for the detection of WWTP effluent plume. Gd shows a good correlation with chloride content and resulted in similar mixing proportions to the ones calculated with CBZ or boron. Other recent studies have reported that Gd is a strong indicator of surface-groundwater interactions and more reliable than most organic tracers (Boester and Rüde, 2020).

The attenuation study of pharmaceutical compounds along the plume could also provide valuable insights into the transfer and fate of CECs within groundwater, while providing efficient tools for monitoring contamination in the sub-surface environment.

CRediT authorship contribution statement

A. Bonnière: Writing – review & editing, Methodology, Investigation. **S. Khaska:** Validation, Supervision, Conceptualization. **C. Le Gal La Salle:** Validation, Supervision, Conceptualization. **P. Louvat:** Validation, Methodology, Formal analysis. **P. Verdoux:** Resources, Investigation.

Declaration of competing interest

The authors declare that they have no known competing financial interests or personal relationships that could have appeared to influence the work reported in this paper.

Data availability

No data was used for the research described in the article.

Acknowledgments

The PhD grant of A. Bonnière was supported by Nîmes Metropole, the UPR CHROME from Université de Nîmes, France and the EPTB Vistre-Vistrenque. The landowners and the stakeholders are gratefully thanked for giving us the access to the boreholes. The authors also wish to thank AIA (Advanced Isotopic Analysis), Pau, France, for the complementary $\delta^{11}B$ analysis, Dr. Guillaume Trommetter for his technical help on gadolinium discussions, and Mrs Felicia Walsh Jean-Baptiste for her help proofreading the article.

Supplementary materials

Supplementary material associated with this article can be found, in the online version, at doi:10.1016/j.watres.2024.121637.

References

Adebowale, T., Surapaneni, A., Faulkner, D., McCance, W., Wang, S., Currell, M., 2019. Delineation of contaminant sources and denitrification using isotopes of nitrate near a wastewater treatment plant in peri-urban settings. Sci. Total Environ. 651, 2701–2711. https://doi.org/10.1016/j.scitotenv.2018.10.146.

Alcalá, F.J., Custodio, E., 2008. Using the Cl/Br ratio as a tracer to identify the origin of salinity in aquifers in Spain and Portugal. J. Hydrol. 359, 189–207. https://doi.org/10.1016/j.jhydrol.2008.06.028.

Archer, E., Petrie, B., Kasprzyk-Hordern, B., Wolfaardt, G.M., 2017. The fate of pharmaceuticals and personal care products (PPCPs), endocrine disrupting contaminants (EDCs), metabolites and illicit drugs in a WWTW and environmental waters. Chemosphere 174, 437–446. https://doi.org/10.1016/j.chemosphere.2017.01.101.

Bau, M., Dulski, P., 1996. Distribution of yttrium and rare-earth elements in the Penge and Kuruman iron-formations, Transvaal Supergroup, South Africa. Precambrian Res. 79, 37–55. https://doi.org/10.1016/0301-9268(95)00087-9.

Bau, M., Schmidt, K., Pack, A., Bendel, V., Kraemer, D., 2018. The European Shale: an improved data set for normalisation of rare earth element and yttrium concentrations in environmental and biological samples from Europe. Appl. Geochem. 90, 142–149. https://doi.org/10.1016/j.apgeochem.2018.01.008.

Bavumiragira, J.P., Ge, J., Yin, H., 2022. Fate and transport of pharmaceuticals in water systems: a processes review. Sci. Total Environ. 823, 153635 https://doi.org/10.1016/j.scitotenv.2022.153635.

Benedicto, A., Labaume, P., Séguret, M., Séranne, M., 1996. Low-angle crustal ramp and basin geometry in the Gulf of Lion passive margin: Oligocene-Aquitanian Vistrenque graben, SE France. Tectonics 15, 1192–1212. https://doi.org/10.1029/96TC01097.

Bi, P., Pei, L., Huang, G., Han, D., Song, J., 2021. Identification of groundwater contamination in a rapidly urbanized area on a regional scale: a new approach of multi-hydrochemical evidences. IJERPH 18, 12143. https://doi.org/10.3390/ijerph182212143.

Blair, B., Nikolaus, A., Hedman, C., Klaper, R., Grundl, T., 2015. Evaluating the degradation, sorption, and negative mass balances of pharmaceuticals and personal care products during wastewater treatment. Chemosphere 134, 395–401. https://doi.org/10.1016/j.chemosphere.2015.04.078.

Boester, U., Rüde, T.R., 2020. Utilize gadolinium as environmental tracer for surface water-groundwater interaction in Karst. J. Contam. Hydrol. 235, 103710 https://doi.org/10.1016/j.jconhyd.2020.103710.

Briand, C., Plagnes, V., Sebilo, M., Louvat, P., Chesnot, T., Schneider, M., Ribstein, P., Marchet, P., 2013. Combination of nitrate (N, O) and boron isotopic ratios with microbiological indicators for the determination of nitrate sources in karstic groundwater. Environ. Chem. 10, 365. https://doi.org/10.1071/EN13036.

Briand, C., Sebilo, M., Louvat, P., Chesnot, T., Vaury, V., Schneider, M., Plagnes, V., 2017. Legacy of contaminant N sources to the NO_3^- signature in rivers: a combined isotopic ($\delta^{15}N$-NO_3^-, $\delta^{18}O$-NO_3^-, $\delta^{11}B$) and microbiological investigation. Sci. Rep. 7, 41703. https://doi.org/10.1038/srep41703.

Brünjes, R., Bichler, A., Hoehn, P., Lange, F.T., Brauch, H.-J., Hofmann, T., 2016. Anthropogenic gadolinium as a transient tracer for investigating river bank filtration. Sci. Total Environ. 571, 1432–1440. https://doi.org/10.1016/j.scitotenv.2016.06.105.

Burri, N.M., Weatherl, R., Moeck, C., Schirmer, M., 2019. A review of threats to groundwater quality in the anthropocene. Sci. Total Environ. 684, 136–154. https://doi.org/10.1016/j.scitotenv.2019.05.236.

Carbon, D., Fabre, G., Volant, P., Fiches, J.-L., Levret, A., Combes, P., 2005. The Nîmes aqueduct in the upper Vistrenque: interdisciplinary analysis of an underground section: aqueducts of Mediterranean Gaul (L'aqueduc de Nîmes dans la haute Vistrenque : analyse interdisciplinaire d'un tronçon souterrain: aqueducs de la Gaule méditerranéenne). Galia 62, 69–86. https://doi.org/10.3406/galia.2005.3221.

Cary, L., Casanova, J., Gaaloul, N., Guerrot, C., 2013. Combining boron isotopes and carbamazepine to trace sewage in salinized groundwater: a case study in Cap Bon, Tunisia. Appl. Geochem. 34, 126–139. https://doi.org/10.1016/j.apgeochem.2013.03.004.

Chalk, P.M., 2020. Natural variations in stable boron isotopes ($\delta^{11}B$) as tracers in terrestrial ecosystems. Isotopes Environ. Health Stud. 56, 335–345. https://doi.org/10.1080/10256016.2020.1773458.

Clara, M., Strenn, B., Kreuzinger, N., 2004. Carbamazepine as a possible anthropogenic marker in the aquatic environment: investigations on the behaviour of carbamazepine in wastewater treatment and during groundwater infiltration. Water Res. 38, 947–954. https://doi.org/10.1016/j.watres.2003.10.058.

Cook, P.G., Herczeg, A.L. (Eds.), 2000. Environmental Tracers in Subsurface Hydrology. Springer US, Boston, MA. https://doi.org/10.1007/978-1-4615-4557-6.

Currell, M., McCance, W., Jones, O.A.H., 2022. Novel molecular tracers for the assessment of groundwater pollution. Curr. Opin. Environ. Sci. Health 26, 100331. https://doi.org/10.1016/j.coesh.2022.100331.

Ebrahimi, P., Barbieri, M., 2019. Gadolinium as an emerging microcontaminant in water resources: threats and opportunities. Geosciences 9, 93. https://doi.org/10.3390/geosciences9020093.

Gaillardet, J., Lemarchand, D., 2018. Boron in the weathering environment. In: Marschall, H., Foster, G. (Eds.), Boron Isotopes, Advances in Isotope Geochemistry. Springer International Publishing, Cham, pp. 163–188. https://doi.org/10.1007/978-3-319-64666-4_7.

Gasser, G., Rona, M., Voloshenko, A., Shelkov, R., Tal, N., Pankratov, I., Elhanany, S., Lev, O., 2010. Quantitative evaluation of tracers for quantification of wastewater contamination of potable water sources. Environ. Sci. Technol. 44, 3919–3925. https://doi.org/10.1021/es100604c.

Green, T.R., Taniguchi, M., Kooi, H., Gurdak, J.J., Allen, D.M., Hiscock, K.M., Treidel, H., Aureli, A., 2011. Beneath the surface of global change: impacts of climate change on groundwater. J. Hydrol. 405, 532–560. https://doi.org/10.1016/j.jhydrol.2011.05.002.

Gros, M., Petrovic, M., Barceló, D., 2008. Analysis of emerging contaminants of municipal and industrial origin. In: Barceló, D., Petrovic, M. (Eds.), Emerging Contaminants from Industrial and Municipal Waste. Springer Berlin Heidelberg, Berlin, Heidelberg, pp. 37–104. https://doi.org/10.1007/698_5_102.

Grosbois, C., Négrel, Ph., Fouillac, C., Grimaud, D., 2000. Dissolved load of the Loire River: chemical and isotopic characterization. Chem. Geol. 170, 179–201. https://doi.org/10.1016/S0009-2541(99)00247-8.

Grossberger, A., Hadar, Y., Borch, T., Chefetz, B., 2014. Biodegradability of pharmaceutical compounds in agricultural soils irrigated with treated wastewater. Environ. Pollut. 185, 168–177. https://doi.org/10.1016/j.envpol.2013.10.038.

Guinoiseau, D., Louvat, P., Paris, G., Chen, J.-B., Chetelat, B., Rocher, V., Guérin, S., Gaillardet, J., 2018. Are boron isotopes a reliable tracer of anthropogenic inputs to rivers over time? Sci. Total Environ. 626, 1057–1068. https://doi.org/10.1016/j.scitotenv.2018.01.159.

Gworek, B., Kijeńska, M., Wrzosek, J., Graniewska, M., 2021. Pharmaceuticals in the soil and plant environment: a review. Water Air Soil Pollut. 232, 145. https://doi.org/10.1007/s11270-020-04954-8.

Hai, F., Yang, S., Asif, M., Sencadas, V., Shawkat, S., Sanderson-Smith, M., Gorman, J., Xu, Z.-Q., Yamamoto, K., 2018. Carbamazepine as a possible anthropogenic marker in water: occurrences, toxicological effects, regulations and removal by wastewater treatment technologies. Water 10, 107. https://doi.org/10.3390/w10020107.

Hassan, W.H., Ghanim, A.A.J., Mahdi, K., Adham, A., Mahdi, F.A., Nile, B.K., Riksen, M., Ritsema, C., 2023. Effect of artificial (Pond) recharge on the salinity and groundwater level in Al-Dibdibba Aquifer in Iraq using treated wastewater. Water 15, 695. https://doi.org/10.3390/w15040695.

Hatje, V., Bruland, K.W., Flegal, A.R., 2016. Increases in anthropogenic gadolinium anomalies and rare earth element concentrations in San Francisco Bay over a 20 year record. Environ. Sci. Technol. 50, 4159–4168. https://doi.org/10.1021/acs.est.5b04322.

Hissler, C., Hostache, R., Iffly, J.F., Pfister, L., Stille, P., 2015. Anthropogenic rare earth element fluxes into floodplains: coupling between geochemical monitoring and hydrodynamic sediment transport modelling. C. R. Geosci. 347, 294–303. https://doi.org/10.1016/j.crte.2015.01.003.

Huang, G., Liu, C., Zhang, Y., Chen, Z., 2020. Groundwater is important for the geochemical cycling of phosphorus in rapidly urbanized areas: a case study in the Pearl River Delta. Environ. Pollut. 260, 114079 https://doi.org/10.1016/j.envpol.2020.114079.

Huang, T., Pang, Z., 2011. Estimating groundwater recharge following land-use change using chloride mass balance of soil profiles: a case study at Guyuan and Xifeng in the Loess Plateau of China. Hydrogeol. J. 19, 177–186. https://doi.org/10.1007/s10040-010-0643-8.

HYDRIAD, 2015. Delimitation study of the Pazac priority catchment area (Commune of Sernhac) and characterisation of its vulnerability to diffuse pollution (Étude de délimitation du bassin d'alimentation du captage prioritaire de Pazac (Commune de Sernhac) et caractérisation de sa vulnérabilité aux pollutions diffuses).

ICH, 2005. Validation of Analytical Procedures: Text and Methodology. International Conference on Harmonization (ICH), Q2(R1).

IPCC, 2023. Climate Change 2022—Impacts, Adaptation and Vulnerability: Working Group II Contribution to the Sixth Assessment Report of the Intergovernmental Panel on Climate Change, first ed. Cambridge University Press. https://doi.org/10.1017/9781009325844.

Jakóbczyk-Karpierz, S., Ślósarczyk, K., 2022. Isotopic signature of anthropogenic sources of groundwater contamination with sulfate and its application to groundwater in a heavily urbanized and industrialized area (Upper Silesia, Poland). J. Hydrol. 612, 128255 https://doi.org/10.1016/j.jhydrol.2022.128255.

Jarraya-Horriche, F., Benabdallah, S., Ayadi, M., 2020. Groundwater monitoring for assessing artificial recharge in the Mediterranean coastal aquifer of Korba (Northeastern Tunisia). Environ. Monit. Assess. 192, 442. https://doi.org/10.1007/s10661-020-08408-w.

Johannesson, K.H., Palmore, C.D., Fackrell, J., Prouty, N.G., Swarzenski, P.W., Chevis, D. A., Telfeyan, K., White, C.D., Burdige, D.J., 2017. Rare earth element behavior during groundwater–seawater mixing along the Kona Coast of Hawaii. Geochim. Cosmochim. Acta 198, 229–258. https://doi.org/10.1016/j.gca.2016.11.009.

Kasprzyk-Hordern, B., Dinsdale, R.M., Guwy, A.J., 2009. The removal of pharmaceuticals, personal care products, endocrine disruptors and illicit drugs during wastewater treatment and its impact on the quality of receiving waters. Water Res. 43, 363–380. https://doi.org/10.1016/j.watres.2008.10.047.

Katz, B.G., Eberts, S.M., Kauffman, L.J., 2011. Using Cl/Br ratios and other indicators to assess potential impacts on groundwater quality from septic systems: a review and examples from principal aquifers in the United States. J. Hydrol. 397, 151–166. https://doi.org/10.1016/j.jhydrol.2010.11.017.

Katz, B.G., Griffin, D.W., Davis, J.H., 2009. Groundwater quality impacts from the land application of treated municipal wastewater in a large karstic spring basin: chemical and microbiological indicators. Sci. Total Environ. 407, 2872–2886. https://doi.org/10.1016/j.scitotenv.2009.01.022.

Khan, N.A., Khan, S.U., Ahmed, S., Farooqi, I.H., Yousefi, M., Mohammadi, A.A., Changani, F., 2020. Recent trends in disposal and treatment technologies of emerging-pollutants—A critical review. TrAC Trends Anal. Chem. 122, 115744 https://doi.org/10.1016/j.trac.2019.115744.

Khasawneh, O.F.S., Palaniandy, P., 2021. Occurrence and removal of pharmaceuticals in wastewater treatment plants. Process Saf. Environ. Protect. 150, 532–556. https://doi.org/10.1016/j.psep.2021.04.045.

Kiecak, A., Sassine, L., Boy-Roura, M., Elsner, M., Mas-Pla, J., Le Gal La Salle, C., Stumpp, C., 2019. Sorption properties and behaviour at laboratory scale of selected pharmaceuticals using batch experiments. J. Contam. Hydrol. 225, 103500 https://doi.org/10.1016/j.jconhyd.2019.103500.

Knappe, A., Möller, P., Dulski, P., Pekdeger, A., 2005. Positive gadolinium anomaly in surface water and ground water of the urban area Berlin, Germany. Geochemistry 65, 167–189. https://doi.org/10.1016/j.chemer.2004.08.004.

Kodešová, R., Kočárek, M., Klement, A., Golovko, O., Koba, O., Fér, M., Nikodem, A., Vondráčková, L., Jakšík, O., Grabic, R., 2016. An analysis of the dissipation of pharmaceuticals under thirteen different soil conditions. Sci. Total Environ. 544, 369–381. https://doi.org/10.1016/j.scitotenv.2015.11.085.

K'oreje, K.O., Vergeynst, L., Ombaka, D., De Wispelaere, P., Okoth, M., Van Langenhove, H., Demeestere, K., 2016. Occurrence patterns of pharmaceutical residues in wastewater, surface water and groundwater of Nairobi and Kisumu city, Kenya. Chemosphere 149, 238–244. https://doi.org/10.1016/j.chemosphere.2016.01.095.

Kulaksız, S., Bau, M., 2011. Anthropogenic gadolinium as a microcontaminant in tap water used as drinking water in urban areas and megacities. Appl. Geochem. 26, 1877–1885. https://doi.org/10.1016/j.apgeochem.2011.06.011.

Kumar, C.P., 2012. Climate change and its impact on groundwater resources. RESEARCH INVENTY: Int. J. Eng. Sci. 1, 43–60.

Ladouche, B., Luc, A., Nathalie, D., 2009. Chemical and isotopic investigation of rainwater in Southern France (1996–2002): potential use as input signal for karst functioning investigation. J. Hydrol. 367, 150–164. https://doi.org/10.1016/j.jhydrol.2009.01.012.

Lapworth, D.J., Baran, N., Stuart, M.E., Ward, R.S., 2012. Emerging organic contaminants in groundwater: a review of sources, fate and occurrence. Environ. Pollut. 163, 287–303. https://doi.org/10.1016/j.envpol.2011.12.034.

Lapworth, D.J., Das, P., Shaw, A., Mukherjee, A., Civil, W., Petersen, J.O., Gooddy, D.C., Wakefield, O., Finlayson, A., Krishan, G., Sengupta, P., MacDonald, A.M., 2018. Deep urban groundwater vulnerability in India revealed through the use of emerging organic contaminants and residence time tracers. Environ. Pollut. 240, 938–949. https://doi.org/10.1016/j.envpol.2018.04.053.

Lawrence, M.G., Bariel, D.G., 2010. Tracing treated wastewater in an inland catchment using anthropogenic gadolinium. Chemosphere 80, 794–799. https://doi.org/10.1016/j.chemosphere.2010.05.001.

Lawrence, M.G., Kamber, B.S., 2006. The behaviour of the rare earth elements during estuarine mixing—Revisited. Mar. Chem. 100, 147–161. https://doi.org/10.1016/j.marchem.2005.11.007.

Lawrence, M.G., Ort, C., Keller, J., 2009. Detection of anthropogenic gadolinium in treated wastewater in South East Queensland, Australia. Water Res. 43, 3534–3540. https://doi.org/10.1016/j.watres.2009.04.033.

Lee, H.-J., Kim, K.Y., Hamm, S.-Y., Kim, M., Kim, H.K., Oh, J.-E., 2019. Occurrence and distribution of pharmaceutical and personal care products, artificial sweeteners, and pesticides in groundwater from an agricultural area in Korea. Sci. Total Environ. 659, 168–176. https://doi.org/10.1016/j.scitotenv.2018.12.258.

Li, X., Atwill, E.R., Antaki, E., Applegate, O., Bergamaschi, B., Bond, R.F., Chase, J., Ransom, K.M., Samuels, W., Watanabe, N., Harter, T., 2015. Fecal indicator and pathogenic bacteria and their antibiotic resistance in alluvial groundwater of an irrigated agricultural region with dairies. J. Environ. Qual. 44, 1435–1447. https://doi.org/10.2134/jeq2015.03.0139.

Li, Z., Yu, X., Yu, F., Huang, X., 2021. Occurrence, sources and fate of pharmaceuticals and personal care products and artificial sweeteners in groundwater. Environ. Sci. Pollut. Res. 28, 20903–20920. https://doi.org/10.1007/s11356-021-12721-3.

Lopez, B., Ollivier, P., Togola, A., Baran, N., Ghestem, J.-P., 2015. Screening of French groundwater for regulated and emerging contaminants. Sci. Total Environ. 518–519, 562–573. https://doi.org/10.1016/j.scitotenv.2015.01.110.

Louis, P., Messaoudene, A., Jrad, H., Abdoul-Hamid, B.A., Vignati, D.A.L., Pons, M.-N., 2020. Understanding Rare Earth Elements concentrations, anomalies and fluxes at the river basin scale: the Moselle River (France) as a case study. Sci. Total Environ. 742, 140619 https://doi.org/10.1016/j.scitotenv.2020.140619.

Louvat, P., Tharaud, M., Buisson, M., Rollion-Bard, C., Benedetti, M.F., 2019. μ-dDIHEN: a new micro-flow liquid sample introduction system for direct injection nebulization in ICP-MS. J. Anal. At. Spectrom. 34, 1553–1563. https://doi.org/10.1039/C9JA00146H.

Mansouri, F., Chouchene, K., Roche, N., Ksibi, M., 2021. Removal of pharmaceuticals from water by adsorption and advanced oxidation processes: state of the art and trends. Appl. Sci. 11, 6659. https://doi.org/10.3390/app11146659.

McArthur, J.M., Sikdar, P.K., Hoque, M.A., Ghosal, U., 2012. Waste-water impacts on groundwater: Cl/Br ratios and implications for arsenic pollution of groundwater in the Bengal Basin and Red River Basin, Vietnam. Sci. Total Environ. 437, 390–402. https://doi.org/10.1016/j.scitotenv.2012.07.068.

McCance, W., Jones, O.A.H., Cendón, D.I., Edwards, M., Surapaneni, A., Chadalavada, S., Currell, M., 2021. Decoupling wastewater impacts from hydrogeochemical trends in impacted groundwater resources. Sci. Total Environ. 774, 145781 https://doi.org/10.1016/j.scitotenv.2021.145781.

McCance, W., Jones, O.A.H., Cendón, D.I., Edwards, M., Surapaneni, A., Chadalavada, S., Wang, S., Currell, M., 2020. Combining environmental isotopes with contaminants of emerging concern (CECs) to characterise wastewater derived impacts on groundwater quality. Water Res. 182, 116036 https://doi.org/10.1016/j.watres.2020.116036.

McCance, W., Jones, O.A.H., Edwards, M., Surapaneni, A., Chadalavada, S., Currell, M., 2018. Contaminants of emerging concern as novel groundwater tracers for delineating wastewater impacts in urban and peri-urban areas. Water Res. 146, 118–133. https://doi.org/10.1016/j.watres.2018.09.013.

Ménillet, F., Palloc, H., 1973. Note on the 1:50,000 geological map of Nîmes (Notice de la carte géologique de Nîmes au 1/50 000).

Merschel, G., Bau, M., Baldewein, L., Dantas, E.L., Walde, D., Bühn, B., 2015. Tracing and tracking wastewater-derived substances in freshwater lakes and reservoirs: anthropogenic gadolinium and geogenic REEs in Lake Paranoá, Brasilia. C. R. Geosci. 347, 284–293. https://doi.org/10.1016/j.crte.2015.01.004.

Millot, R., Petelet-Giraud, E., Guerrot, C., Négrel, P., 2010. Multi-isotopic composition (δ^7Li–δ^{11}B–δD–δ^{18}O) of rainwaters in France: origin and spatio-temporal characterization. Appl. Geochem. 25, 1510–1524. https://doi.org/10.1016/j.apgeochem.2010.08.002.

Misra, A.K., 2014. Climate change and challenges of water and food security. Int. J. Sustain. Built Environ. 3, 153–165. https://doi.org/10.1016/j.ijsbe.2014.04.006.

Möller, P., Dulski, P., Bau, M., Knappe, A., Pekdeger, A., Sommer-von Jarmersted, C., 2000. Anthropogenic gadolinium as a conservative tracer in hydrology. J. Geochem. Explor. 69–70, 409–414. https://doi.org/10.1016/S0375-6742(00)00083-2.

Morin-Crini, N., Lichtfouse, E., Liu, G., Balaram, V., Ribeiro, A.R.L., Lu, Z., Stock, F., Carmona, E., Teixeira, M.R., Picos-Corrales, L.A., Moreno-Piraján, J.C., Giraldo, L., Li, C., Pandey, A., Hocquet, D., Torri, G., Crini, G., 2022. Worldwide cases of water pollution by emerging contaminants: a review. Environ. Chem. Lett. https://doi.org/10.1007/s10311-022-01447-4.

Négrel, P., Millot, R., Guerrot, C., Petelet-Giraud, E., Brenot, A., Malcuit, E., 2012. Heterogeneities and interconnections in groundwaters: coupled B, Li and stable-isotope variations in a large aquifer system (Eocene Sand aquifer, Southwestern France). Chem. Geol. 296–297, 83–95. https://doi.org/10.1016/j.chemgeo.2011.12.022.

Panno, S.V., Hackley, K.C., Hwang, H.H., Greenberg, S.E., Krapac, I.G., Landsberger, S., O'Kelly, D.J., 2006. Characterization and identification of Na-Cl sources in ground water. Ground Water 44, 176–187. https://doi.org/10.1111/j.1745-6584.2005.00127.x.

Pantel, J., 2009. Nitrate transfer in the Vistrenque basin. Modelling approach (Le transfert des nitrates dans le bassin de la Vistrenque. Approche par modélisation). Géologues, Pollution des aquifères par les nitrates et pesticides 9.

Pantel, J., 2000. Etude et modélisation des coupalges entre l'hydrodynamique et les mécanisques de transfert de pollutions azotées en milieu alluvial fortement hétérogène. Nappe de la Vistrenque (Gard) (Terre solide, Géodynamique, Paléobiosphère). Université Montpellier II, Montpellier.

Poul, X., Bayer, F., Buard, C., 1975. Hydrogeological study of the Costière - Vistrenque (Gard) - Report n°1 (Étude hydrogéologique de la Costière - Vistrenque (Gard) - Rapport n°1) (No. 75 SGN 220 LRO). Bureau de Recherches Géologiques et Minières (BRGM), Montpellier.

Rabiet, M., Brissaud, F., Seidel, J.L., Pistre, S., Elbaz-Poulichet, F., 2009. Positive gadolinium anomalies in wastewater treatment plant effluents and aquatic environment in the Hérault watershed (South France). Chemosphere 75, 1057–1064. https://doi.org/10.1016/j.chemosphere.2009.01.036.

Richardson, S.D., DeMarini, D.M., Kogevinas, M., Fernandez, P., Marco, E., Lourencetti, C., Ballesté, C., Heederik, D., Meliefste, K., McKague, A.B., Marcos, R., Font-Ribera, L., Grimalt, J.O., Villanueva, C.M., 2010. What's in the pool? A comprehensive identification of disinfection by-products and assessment of mutagenicity of chlorinated and brominated swimming pool water. Environ. Health Perspect. 118, 1523–1530. https://doi.org/10.1289/ehp.1001965.

Sassine, L., 2014. Occurrence of pesticides and emerging contaminants in alluvial groundwater. Constraints imposed by the origin and residence time of the water. The case of the Vistrenque aquifer (Occurrence des pesticides et des contaminants émergents dans une nappe alluviale. Contraintes apportées par l'origine et le temps de résidence de l'eau. Cas de la nappe de la Vistrenque) (Hydrogéochimie isotopique). Université d'Aix-Marseille.

Sassine, L., Khaska, M., Ressouche, S., Simler, R., Lancelot, J., Verdoux, P., Le Gal La Salle, C., 2015. Coupling geochemical tracers and pesticides to determine recharge origins of a shallow alluvial aquifer: case study of the Vistrenque hydrogeosystem

(SE France). Appl. Geochem. 56, 11–22. https://doi.org/10.1016/j.apgeochem.2015.02.001.
Sassine, L., Le Gal La Salle, C., Khaska, M., Verdoux, P., Meffre, P., Benfodda, Z., Roig, B., 2017. Spatial distribution of triazine residues in a shallow alluvial aquifer linked to groundwater residence time. Environ. Sci. Pollut. Res. 24, 6878–6888. https://doi.org/10.1007/s11356-016-7224-x.
Schmitt, A.-D., Vigier, N., Lemarchand, D., Millot, R., Stille, P., Chabaux, F., 2012. Processes controlling the stable isotope compositions of Li, B, Mg and Ca in plants, soils and waters: a review. C. R. Geosci. 344, 704–722. https://doi.org/10.1016/j.crte.2012.10.002.
Seiler, R.L., 2005. Combined use of 15N and 18O of nitrate and 11B to evaluate nitrate contamination in groundwater. Appl. Geochem. 20, 1626–1636. https://doi.org/10.1016/j.apgeochem.2005.04.007.
Séranne, M., Benedicto, A., Labaume, P., Truffert, C., Pascal, G., 1995. Structural style and evolution of the Gulf of Lion Oligo-Miocene rifting: role of the Pyrenean orogeny. Mar. Pet. Geol. 12, 809–820.
Sérodes, J.-B., Behmel, S., Simard, S., Laflamme, O., Grondin, A., Beaulieu, C., Proulx, F., Rodriguez, M.J., 2021. Tracking domestic wastewater and road de-icing salt in a municipal drinking water reservoir: acesulfame and chloride as co-tracers. Water Res. 203, 117493 https://doi.org/10.1016/j.watres.2021.117493.
Sui, Q., Cao, X., Lu, S., Zhao, W., Qiu, Z., Yu, G., 2015. Occurrence, sources and fate of pharmaceuticals and personal care products in the groundwater: a review. Emerg. Contam. 1, 14–24. https://doi.org/10.1016/j.emcon.2015.07.001.
Torssander, P., Mörth, C.-M., Kumpulainen, R., 2006. Chemistry and sulfur isotope investigation of industrial wastewater contamination into groundwater aquifers, Piteå County, N. Sweden. J. Geochem. Explor. 88, 64–67. https://doi.org/10.1016/j.gexplo.2005.08.016.
Trommetter, G., Dumoulin, D., Dang, D.H., Alaimo, V., Billon, G., 2022. On inorganic tracers of wastewater treatment plant discharges along the Marque River (Northern France). Chemosphere 305, 135413. https://doi.org/10.1016/j.chemosphere.2022.135413.
US EPA, 2012. Water: Contaminant Candidate List 3. US. Environmental Protection Agency, Washington, DC.
US EPA, 2008. Aquatic life criteria for contaminants of emerging concern. US. Environmental Protection Agency, Washington, DC.
Van Stempvoort, D.R., Roy, J.W., Grabuski, J., Brown, S.J., Bickerton, G., Sverko, E., 2013. An artificial sweetener and pharmaceutical compounds as co-tracers of urban wastewater in groundwater. Sci. Total Environ. 461–462, 348–359. https://doi.org/10.1016/j.scitotenv.2013.05.001.
Vengosh, A., Heumann, K.G., Juraske, S., Kasher, R., 1994. Boron isotope application for tracing sources of contamination in groundwater. Environ. Sci. Technol. 28, 1968–1974. https://doi.org/10.1021/es00060a030.
Vengosh, A., Pankratov, I., 1998. Chloride/bromide and chloride/fluoride ratios of domestic sewage effluents and associated contaminated ground water. Ground Water 36, 815–824. https://doi.org/10.1111/j.1745-6584.1998.tb02200.x.
Verlicchi, P., Al Aukidy, M., Zambello, E., 2012. Occurrence of pharmaceutical compounds in urban wastewater: removal, mass load and environmental risk after a secondary treatment—A review. Sci. Total Environ. 429, 123–155. https://doi.org/10.1016/j.scitotenv.2012.04.028.
Widory, D., Petelet-Giraud, E., Négrel, P., Ladouche, B., 2005. Tracking the sources of nitrate in groundwater using coupled nitrogen and boron isotopes: a synthesis. Environ. Sci. Technol. 39, 539–548. https://doi.org/10.1021/es0493897.
Wilkinson, J.L., Boxall, A.B.A., Kolpin, D.W., Leung, K.M.Y., Lai, R.W.S., Galbán-Malagón, C., Adell, A.D., Mondon, J., Metian, M., Marchant, R.A., Bouzas-Monroy, A., Cuni-Sanchez, A., Coors, A., Carriquiriborde, P., Rojo, M., Gordon, C., Cara, M., Moermond, M., Luarte, T., Petrosyan, V., Perikhanyan, Y., Mahon, C.S., McGurk, C.J., Hofmann, T., Kormoker, T., Iniguez, V., Guzman-Otazo, J., Tavares, J. L., Gildasio De Figueiredo, F., Razzolini, M.T.P., Dougnon, V., Gbaguidi, G., Traoré, O., Blais, J.M., Kimpe, L.E., Wong, M., Wong, D., Ntchantcho, R., Pizarro, J., Ying, G.-G., Chen, C.-E., Páez, M., Martínez-Lara, J., Otamonga, J.-P., Poté, J., Ifo, S. A., Wilson, P., Echeverría-Sáenz, S., Udikovic-Kolic, N., Milakovic, M., Fatta-Kassinos, D., Ioannou-Ttofa, L., Belušová, V., Vymazal, J., Cárdenas-Bustamante, M., Kassa, B.A., Garric, J., Chaumot, A., Gibba, P., Kunchulia, I., Seidensticker, S., Lyberatos, G., Halldórsson, H.P., Melling, M., Shashidhar, T., Lamba, M., Nastiti, A., Supriatin, A., Pourang, N., Abedini, A., Abdullah, O., Gharbia, S.S., Pilla, F., Chefetz, B., Topaz, T., Yao, K.M., Aubakirova, B., Beisenova, R., Olaka, L., Mulu, J. K., Chatanga, P., Ntuli, V., Blama, N.T., Sherif, S., Aris, A.Z., Looi, L.J., Niang, M., Traore, S.T., Oldenkamp, R., Ogunbanwo, O., Ashfaq, M., Iqbal, M., Abdeen, Z., O'Dea, A., Morales-Saldaña, J.M., Custodio, M., de la Cruz, H., Navarrete, I., Carvalho, F., Gogra, A.B., Koroma, B.M., Cerkvenik-Flajs, V., Gombač, M., Thwala, M., Choi, K., Kang, H., Ladu, J.L.C., Rico, A., Amerasinghe, P., Sobek, A., Horlitz, G., Zenker, A.K., King, A.C., Jiang, J.-J., Kariuki, R., Tumbo, M., Tezel, U., Onay, T.T., Lejju, J.B., Vystavna, Y., Vergeles, Y., Heinzen, H., Pérez-Parada, A., Sims, D.B., Figy, M., Good, D., Teta, C., 2022. Pharmaceutical pollution of the world's rivers. Proc. Natl. Acad. Sci. USA 119, e2113947119. https://doi.org/10.1073/pnas.2113947119.